Pharmacological Research 165 (2021) 105434

Contents lists available at ScienceDirect

Pharmacological Research

journal homepage: www.elsevier.com/locate/yphrs

Prolonged dopamine D_3 receptor stimulation promotes dopamine transporter ubiquitination and degradation through a PKC-dependent mechanism

Diego Luis-Ravelo [a,b,1], Felipe Fumagallo-Reading [a,b,1], Javier Castro-Hernandez [a], Pedro Barroso-Chinea [a,b], Domingo Afonso-Oramas [a,b], Alejandro Febles-Casquero [a], Ignacio Cruz-Muros [a,b], Josmar Salas-Hernandez [a,b], Virginia Mesa-Infante [a], Julia Rodriguez-Nuñez [a], Tomas Gonzalez-Hernandez [a,b,*]

[a] Departamento de Ciencias Médicas Básicas, Facultad de Medicina, Universidad de La Laguna, Tenerife, Spain
[b] Instituto de Tecnologías Biomédicas (ITB), Universidad de La Laguna, Tenerife, Spain

ARTICLE INFO

Keywords:
Dopaminergic neurons
Autoreceptors
Down-regulation
Parkinson's disease
Depression

Chemical compounds studied in this article:
Pramipexole dihydrochloride (PubChem CID:166589)
7-OH-DPAT (PubChem CID: 1219)
L741,626 (PubChem CID: 133633)
NGB2904 (PubChem CID: 189060-98-8)

ABSTRACT

The dopamine transporter (DAT) is a membrane glycoprotein in dopaminergic neurons, which modulates extracellular and intracellular dopamine levels. DAT is regulated by different presynaptic proteins, including dopamine D_2 (D_2R) and D_3 (D_3R) receptors. While D_2R signalling enhances DAT activity, some data suggest that D_3R has a biphasic effect. However, despite the extensive therapeutic use of D_2R/D_3R agonists in neuropsychiatric disorders, this phenomenon has been little studied. In order to shed light on this issue, DAT activity, expression and posttranslational modifications were studied in mice and DAT-D_3R-transfected HEK cells. Consistent with previous reports, acute treatment with D_2R/D_3R agonists promoted DAT recruitment to the plasma membrane and an increase in DA uptake. However, when the treatment was prolonged, DA uptake and total striatal DAT protein declined below basal levels. These effects were inhibited in mice by genetic and pharmacological inactivation of D_3R, but not D_2R, indicating that they are D_3R-dependent. No changes were detected in mesostriatal tyrosine hydroxylase (TH) protein expression and midbrain TH and DAT mRNAs, suggesting that the dopaminergic system is intact and DAT is posttranslationally regulated. The use of immunoprecipitation and cell surface biotinylation revealed that DAT is phosphorylated at serine residues, ubiquitinated and released into late endosomes through a PKCβ-dependent mechanism. In sum, the results indicate that long-term D_3R activation promotes DAT down-regulation, an effect that may underlie neuroprotective and antidepressant actions described for some D_2R/D_3R agonists.

1. Introduction

Dopamine (DA) neurotransmission plays an essential role in the control of locomotor activity, reward-associated behaviour and cognition [1,2]. The spatial and temporal strength of DA signalling is determined to a large extent by the action of the DA transporter (DAT), a plasma membrane glycoprotein selectively expressed in dopaminergic neurons that mediates the uptake of released DA into presynaptic terminals [3]. Abnormal DAT function has been associated with neurodegenerative and psychiatric conditions such as Parkinson's disease, bipolar disorder, depression and attention deficit hyperactivity disorder [4,5]. In addition, DAT is the target for addictive psychostimulants that inhibit the uptake of DA, reinforcing its actions on postsynaptic receptors [6]. DAT activity is regulated by the action of different signalling systems, including ERK, PI3K and PKC, as well as interaction with presynaptic proteins such as α-synuclein, syntaxin 1A and DA D_2 and D_3 autoreceptors, that promote either DAT plasma membrane stability or internalization [4,7–9]. DA receptors are

Abbreviations: BIM, bisindolylmaleimide; CHX, cycloheximide; DA, dopamine; DAT, dopamine transporter; D_2R, dopamine D_2 receptor; D_3R, dopamine D_3 receptor; PLA, proximity ligation assay; PKC, protein kinase C; PPX, pramipexole.

* Corresponding autor at: Departamento de Ciencias Médicas Básicas, Facultad de Medicina, Universidad de La Laguna, Tenerife, Spain.
E-mail address: tgonhern@ull.edu.es (T. Gonzalez-Hernandez).

[1] These authors contributed equally to this work.

https://doi.org/10.1016/j.phrs.2021.105434
Received 22 July 2020; Received in revised form 17 December 2020; Accepted 6 January 2021
Available online 20 January 2021

classified into two major groups that differ in their signaling profile. D1-like (D1 and D5) receptors which activate neuronal signaling through adenylyl cyclase and the increase of cAMP levels, and D2-like (D2, D3 and D4) receptors which inhibit adenylyl cyclase, reducing cAMP levels [10,11]. While D1-like and D4 receptors are expressed only in non-dopaminegic neurons [10,12], D2 (D_2R) and D3 (D_3R) receptors are also expressed in dopaminergic neurons where they act as DA sensors regulating DA synthesis, release and uptake in response to extracellular DA levels [8,9,13,14]. The transport of DA is increased or decreased in the mouse striatum after a single injection of DA D_2/D_3 receptor (D_2R/D_3R) agonists or antagonists, respectively [15–18]. Likewise, a few minutes treatment with DA receptor agonists promotes DAT recruitment to the plasma membrane and DA uptake in D_2R-DAT [19,20] and D_3R-DAT cotransfected cells [21]. Some reports also suggest that after prolonged treatment with D_2R/D_3R agonists, DA uptake declines below basal levels [22,23]. However, despite D2R/D3R ligands being extensively used as long-term treatment in Parkinson's disease and other neurological conditions, this phenomenon has been much less studied.

The close homology between D_2R and D_3R, sharing 75 % of amino acid sequence in their transmembrane domains, has made the design of selective ligands, particularly D_2R and D_3R agonists, a challenging task (Missale et al., 1998; Beaulieu and Gainetdinov, 2011). So, although some compounds have a moderately higher affinity for D_2R or D_3R, it is still more appropriate to use the term D_2R/D_3R agonists. D_2R/D_3R agonists are extensively used in the treatment of Parkinson's disease to relieve motor symptoms associated with striatal DA deficit [24–26]. The D_2R/D_3R agonist pramipexole (PPX) has also proved to be an effective therapy in treatment-resistant depression and bipolar disorder [27–29]. Given the implication of DA handling in the pathophysiology of these conditions [2,5,30], DA uptake modulation might be involved in the therapeutic effects of D_2R/D_3R agonists. In order to gain further insight into this issue, here we investigated the effect of prolonged D_2R/D_3R agonist treatment on DA uptake and DAT expression using wild-type and D_2RKO and D_3RKO mice, and DAT-D_3R transfected cells. The results reveal an initial recruitment of DAT to the plasma membrane with an increase in DA uptake, but when D_2R/D_3R agonist treatment is prolonged, DA uptake falls below basal levels, and DAT undergoes phosphorylation, ubiquitination and degradation. This effect is mediated by D_3R through a PKCβ-dependent mechanism.

2. Material and methods

2.1. Mice

The experiments were carried out on 22−24 g (4–6 months old) male C57BL/6 J, DA D_3 receptor knockout mice (D_3RKO; B6.129S4-Drd3^{tm1Dac}/J), and D_2RKO (B6.129S2-Drd2^{tm1Low}/J) mice and their wild-type (WT) littermates. D_3RKO mice were obtained from the Jackson Laboratory, and generated on a pure C57BL/6 J genetic background [31,32]. The D_2RKO mice were generated by homologous recombination as previously described [33]. D_2RKO mice and their WT littermates were obtained by mating heterozygous mice [34]. Genotype was determined by polymerase chain reaction. Experimental protocols were approved by the Ethical Committee of the University of La Laguna (#CEIBA2013−0083), and are in accordance with the European Communities Council Directive of 22 September 2010 (2010/63/EU) and ARRIVE guidelines regarding the care and use of animals for scientific purposes. Animals were housed in groups of 3–4 per cage, in conditions of constant temperature (21–22 °C), a 12 h light/dark cycle, and given free access to standard chow and water. Intraperitoneal injections were performed between 3 pm and 4 pm using a small syringe with a 29 G needle. No additional medications were given to reduce suffering because the compounds and volumes injected do not elicit pain. Mice receiving prolonged treatment were sacrificed between 10 a.m. and 12 a.m. The total number of mice used was 181, with each experimental group consisting of 5–6 arbitrarily selected mice.

2.2. DAT and D_3R expression

HEK293 cells were obtained from the European Collection of Cell Cultures (ECACC #85120602) and used without further authentication. They were cultured in Dulbecco's Modified Eagle's Medium (DMEM; #L0104; Biowest, Riverside, MO) supplemented with 10 % fetal bovine serum (FBS; #S1810; Biowest) and 1% antibiotics (penicillin 100U/mL and 100 μg/mL streptomycin; #L0018; Biowest). Cultures were maintained in a humidified incubator set at 37 °C and 5% CO_2. Stable cells expressing rat DAT were obtained as described in Afonso-Oramas et al. [35].

Semiconfluent DAT-HEK cells were transfected with pCEP4-EGFP-hDRD3 using Lipofectamine 2000 (#11668; Thermo Fisher Scientific, Walthman, MA) at a ratio of 2:1 according to the manufacturer's protocol. The plasmid was a gift from Dr. Jean-Michel Arrang (Addgene plasmid ♯24098). Stable cell lines expressing EGFP-hD_3R were obtained by growth in selective medium containing 400 μg/mL hygromycin B (#10687010; Thermo Fisher). After 8–10 days of selection, individual clones were expanded in multi-well plates and screened for expression by immunofluorescence and western blot for GFP. Several positive clones were identified and used for subsequent experiments. Subconfluent cultures of DAT-D_3R-HEK cells were grown and treated with dopamine receptor agonists. Cells were subjected to a maximum of ten passages throughout the study. All experiments were performed in triplicate.

2.3. Treatment

Mice and cells were treated with the D_2R/D_3R preferential agonist pramipexole (pramipexole dihydrochloride, PPX (CID:166589, #1237; Sigma; half-life of 8−12 hours). In order to establish what the effective PPX dose was on DAT activity, WT mice received a single intraperitoneal injection of PPX in the range of 0.05–1.5 mg/kg or its vehicle (50 μL 0.9 % sterile saline) and were sacrificed 30 min later, and DAT-D_3R HEK cells were incubated in 0.1−100 μM PPX for 5 min. In some experiments, cells were treated with 7-OH-DPAT (CID: 1219; #H865; Sigma), another D_2R/D_3R agonist that also has 7-fold higher affinity for D_3R than for D_2R [36]. Following Everett and Senogles [37], 7-OH-DPAT was used at a concentration of 0.1 μM. Furthermore, the selective D_2R antagonist L741,626 (CID: 133633; #L135; Sigma; 1 mg/kg, s.c.) or the selective D_3R antagonist NGB2904 (CID: 189060-98-8; #2635; R & D Systems, Minneapolis, MN; 1 mg/kg, i.p.), or their vehicle (0.05 % lactic acid, #L1750, s.c.; Sigma, or 25 % w/v 2-Hydroxypropyl-β-cyclodextrin, #H107, i.p; Sigma, respectively; 50 μL) were injected 30 min before PPX in a group of mice. NGB2904 (10 μM) and the protein synthesis inhibitor cycloheximide (#C4859; Sigma; 20 μM) were also added to the medium 30 and 45 min before PPX, respectively, in some cell experiments.

2.4. DAT antibodies

Different commercial anti-DAT antibodies against C- and N-terminal fragments of human and rat DAT have been tested in our laboratory using brain samples of different mammalians and cells transfected with wild type and mutated DAT forms [23,35,38,39]. In order to confirm their specificity and sensitivity, and which of them provides better efficiency in the different techniques further tests have been performed (see supplementary Fig.1). According to the results of these tests, a goat polyclonal anti-DAT antibody (#SC1433; Santa Cruz Biotechnology, Santa Cruz, CA) was used for immunohistochemistry and western-blot, a rat monoclonal anti-DAT antibody (#MAB369; Millipore, Billerica, MA) for immunoprecipitation, and a rabbit polyclonal anti-DAT (#D6944, Sigma) for *in situ* proximity ligation assay.

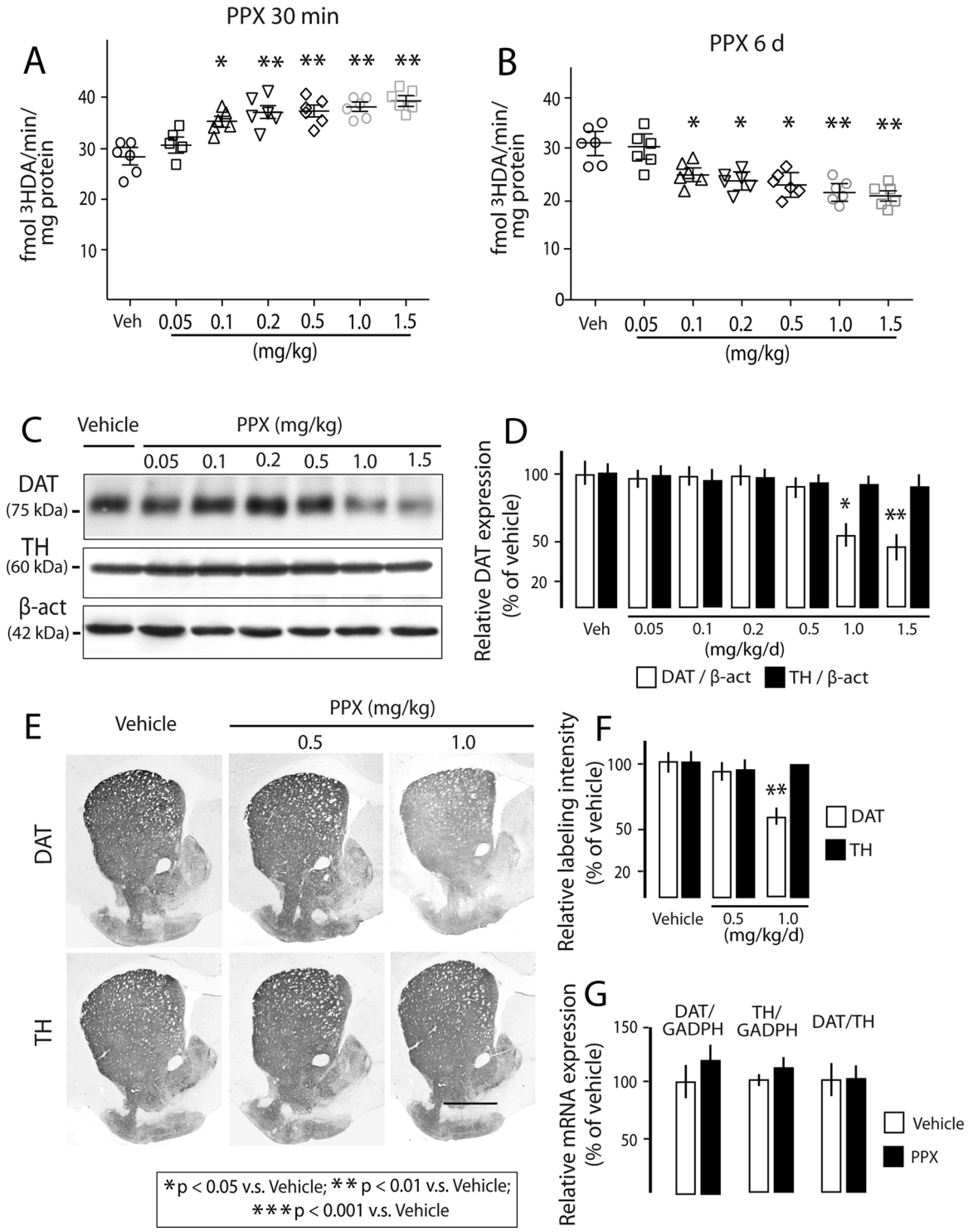

Fig. 1. DAT is regulated in a time-dependent manner by the D_2R/D_3R agonist pramipexole in mouse striata. (A, B) DA uptake in mouse striata after acute (A; 30 min after a single injection) and prolonged treatment (B; 6 days of treatment) with different doses of pramipexole (PPX; 0.05-1.5 mg/kg; n = 6 mice per condition). At PPX doses ≥ 0.1 mg/kg, DA uptake increases after acute treatment and decreases after prolonged treatment (*p < 0.05, ** p < 0.01 vs. Vehicle; Kruskal-Wallis test followed by Dunn's multiple comparison test). (C-F) Western-blot (C, D; n = 4 mice per condition) and immunohistochemistry (E, F; n = 5 mice per condition) for DAT and TH in mouse striata after prolonged treatment with different doses of PPX. DAT expression (* p < 0.05; ** p < 0.01 vs. Vehicle), but not TH expression (p = 0.52 in Western-blot, p = 0.49 in immunohistochemistry; Kruskal-Wallis test followed by Dunn's multiple comparison test), decreases at PPX doses ≥ 1 mg/kg. (G) Quantitative RT-PCR for DAT mRNA and TH mRNA in the ventral midbrain of mice after 6 days of treatment with 1 mg/kg PPX (n = 6 mice per condition; Mann-Whitney test). Relative expression of TH mRNA and DAT mRNA was normalized to GADPH mRNA and calculated as previously described by Pfaffl [41]. Inasmuch as TH mRNA was not modified by PPX (p = 0.57), DAT mRNA was normalized to TH mRNA expression. No differences were found in DAT mRNA levels between vehicle and PPX treated mice (p = 0.85). Data are presented as means ± SEM. β-act, β-actin; Bar in E, 1 mm.

2.5. Western-blot in whole extracts and plasma membranes

Mice were deeply anaesthetized with an overdose of sodium pentobarbital (#P3741; Sigma, St. Louis, MO) and striata were dissected in ice from freshly obtained brains with the aid of an acrylic brain slicer (#PA002; David Kopf Instruments, CA). Whole protein extracts were obtained in M-PER (#78501; Thermo Fisher) with protease (#1169498001; Roche, Basel, Switzerland) and phosphatase inhibitors (#04906845001; Roche). After sonication (3 bursts of 5 s in ice), striatal lysates were centrifuged at 17,000 xg for 5 min and the supernatants were collected. HEK cells were washed in PBS and harvested by scraping. Cell suspensions were centrifuged for 5 min at 1,000 xg, the pellets were washed in PBS twice and resuspended in M-PER.

For biotinylation experiments, synaptosomes were obtained following the impermeant biotinylation procedure [23,35]. Striatal samples were immediately homogenized in 20 vol of ice-cold sucrose bicarbonate solution (SBS, 320 mM sucrose (#S0385; Sigma) in 5 mM sodium bicarbonate (#S5761; Sigma), pH 7.4) with 12 up and down strokes in a Teflon-glass homogenizer. The homogenates were centrifuged (1000 x g, 10 min, 4 °C), and the pellets (P1) containing nuclei and large debris discarded. The supernatants (S1) were centrifuged (17,000 x g, 20 min, 4 °C), and the pellets (P2) were resuspended in 500 µL ice-cold assay buffer [125 mM NaCl (#1.06404; Merck, Darmstadt, Germany), 5 mM KCl (#131494.1210; Panreac), 1.5 mM $MgSO_4$ (#5886; Merck), 1.25 mM $CaCl_2$ (#449709; Sigma), 1.5 mM KH_2PO_2 (#131509; Panreac), 10 mM glucose (#G8270; Sigma), 25 mM HEPES (#H3375; Sigma), 0.1 mM EDTA (#EDS; Sigma), 0.1 mM pargyline (#P8013; Sigma) and 0.1 mM ascorbic acid (#A5960; Sigma)]. HEK cells were washed twice in PBS and harvested by adding cold PBS. Cells and Synaptosomes (300 µg total protein) were incubated for 1 h at 4 °C with continual shaking in 500 µl of 1.5 mg/mL sulfo-NHS-biotin (#21326; Thermo Fisher) in PBS/Ca/Mg buffer (138 mM Na Cl, 2.7 mM kCl, 1.5 mM KH_2PO_2, 9.6 mM Na_2HPO_4 (#6580; Merck) 1 mM $MgCl_2$ (#141396; Panreac), 0.1 mM $CaCl_2$, pH 7.3) and centrifuged (8, 000 *g*, 4 min, 4 °C). In order to remove biotinylating reagents, the resulting pellets were resuspended in 1 mL ice-cold 100 mM glycine (#A1067; Panreac) in PBS/Ca/Mg buffer and centrifuged (8,000 xg, 4 min, 4 °C). The resuspension and centrifugation steps were repeated. Final pellets were resuspended again in 1 mL ice-cold 100 mM glycine in PBS/Ca/Mg buffer and incubated for 30 min at 4 °C. Samples were washed three times in PBS/Ca/Mg buffer, and then lysed by sonication for 2–4 seconds in 300 µl Triton X-100 buffer [10 mM Tris-HCl, pH 7.4, 150 mM NaCl, 1 mM EDTA, 1 %Triton X-100 (#9002-913; TX-100, Sigma)] containing protease inhibitors. After incubation in continuous shaking (30 min, 4 °C), the lysates were centrifuged (18,000 x g, 30 min, 4 °C), and the supernatants were incubated with monomeric avidin bead (#20228; Thermo Fisher) - Triton X-100 buffer (100 µl) for 1 h at RT, and centrifuged (18,000 g, 4 min, 4 °C). The resulting pellets (containing avidin-absorbed biotinylated surface proteins) were resuspended in 1 mL Triton X-100 buffer and centrifuged (18,000 x g, 4 min, 4 °C). Resuspension and centrifugation were repeated two more times, and the final pellets were stored.

Proteins were quantified using the bicinchoninic acid (#B9643; Sigma) method and bovine serum albumin (BSA, #A1391; Panreac, Barcelona, Spain) as standard. Protein samples were diluted in Laemmli's loading buffer [62.5 mM Tris-HCl, 20 % glycerol (#G7757; Sigma), 2% sodium dodecyl sulphate (SDS, #L3771; Sigma), 1.7 % β-mercaptoethanol (#6250, Sigma) and 0.05 % bromophenol blue (#B5525; Sigma), pH 6.8], denatured (90 °C, 5 min.), separated by electrophoresis in 10 % SDS-polyacrylamide gel, and transferred to nitrocellulose (#1620115; Schleicher&Schuell, Dassel, Germany). Blots were blocked for 2 h at RT with 5% non-fat dry milk, and incubated overnight at 4 °C in blocking solution with goat polyclonal anti-DAT Santa Cruz Biotechnology; 1:5,000) or mouse monoclonal anti-tyrosine hydroxylase (TH; #T2928; Sigma;1:30,000;). After several rinses in TBST-5% milk, the membranes were incubated for 1 h in peroxidase conjugated anti-goatIgG (#107013; Jackson-Immunoresearch; 1:50,000) or peroxidase conjugated anti-mouseIgG (#115-035-146; Jackson-Immunoresearch; 1: 50,000). After processing, each nitrocellulose membrane was reblotted for different sample loading markers: β-Actin (#A5441; Sigma; 1: 50,000) or α-Tubulin (#T6074; Sigma; 1: 30,000) in the case of whole protein extracts, plasma membrane Ca^{2+} ATPase 2 (PMCA2; #PA1−915, Thermo Fisher; 1:5,000) in the case of synaptosomal membranes, and calnexin in the case of cytosolic extracts (#4731, Sigma; 1: 4,000). Each TH and DAT immunoreactive band was compared with its loading control. Different protein quantities, antibody dilutions and exposure times were tested to establish their working range. Immunoreactive bands were visualized using enhanced chemiluminiscence (Immun-Star, #1705061; Bio-Rad, CA) and a Chemi-Doc imaging system (#12003153; Bio-Rad). The labelling densities were quantified using a densitometry software (Image Lab 5.2; Bio-Rad). A rectangle of uniform size and shape was placed over each band, and the density values were calculated by subtracting the background at approximately 2 mm above each band. The origin of protein extract was blinded for the quantitative analysis of western-blot images. Data are expressed as a percentage of the mean labelling intensity in basal conditions ± SEM.

2.6. Immunostaining

Mice were deeply anaesthetized with an overdose of sodium pentobarbital and transcardially perfused with heparinized ice-cold 0.9 % saline (20 mL) followed by 4% paraformaldehyde (#818715; Sigma) in phosphate buffered saline 0.1 M pH 7.4 (PBS, 50 mL). The brains were removed and stored overnight in the same fixative at 4 °C, cryoprotected in 30 % (w/v) sucrose -PBS solution and stored at –80 °C until processing. Coronal sections (25 µm) were obtained with a freezing microtome (Thermo Fisher), collected in 6–8 parallel series and processed for DAT immunohistochemistry [34,35]. Floating sections were immersed for 30 min in 3% H_2O_2 (#216763; Sigma) to inactivate endogenous peroxidase, and incubated for 60 min at room temperature (RT) in 4% normal donkey serum (#017-000-001; NDS, Jackson ImmunoResearch, West Grove, PA), or 4% normal goat serum (#005-000-001; NGS, Jackson ImmunoResearch) in PBS, containing 0.05 % Triton X-100, and left overnight in PBS containing 2% NDS and goat anti-DAT polyclonal antibody (Santa Cruz Biotechnology; 1:2,000) or 2% NGS and mouse monoclonal anti-TH (Sigma; 1:10,000). After several rinses, the sections were incubated for 2 h in biotinylated donkey anti-goat antiserum (#705-065-143; Jackson ImmunoResearch; 1:1000) and 1:200 NDS, or goat anti-mouse antiserum (#115-065-003; Jackson ImmunoResearch; 1:1000) and 1:200 NGS in PBS, respectively. Immunoreactions were visible after incubation for 1 h at RT in ExtrAvidin-peroxidase (#E2886; Sigma; 1:200) in PBS, and after 10 min in 0.005 % 3′-3′-diaminobenzidine tetrahydrochloride (#D5637; DAB, Sigma) and 0.001 % H_2O_2 in PBS. The labeling intensity of striatal terminals was quantified following the densitometry procedure previously described [40]. All sections were simultaneously processed using the same protocol and chemical reagents. Microscopic images were digitalized using a Leica DMR trinocular microscope (Leica Microsystems, Wetzlar, Germany). All microscopic and computer parameters were kept constant throughout the densitometric study. Square areas of 100µm × 100µm were randomly selected in the dorsal striatum (8 areas per section, 6 sections 75 µm away from each other, and 5 mice per group). The labeling intensity was quantified using the ImageJ standard program (RRID: SCR_003070). The labeling of each area was defined as the index of light attenuation with respect to the background (neighbouring corpus callosum) and expressed as a percentage of the mean ± S.E.M intensity (arbitrary units, range 0–255) in the control group.

DAT- and DAT-D_3R HEK cells were fixed in 4% paraformaldehyde in PBS for 20 min at RT. Thereafter, they were permeabilized with 0.3 % Triton X-100 in PBS containing 1% bovine serum albumin (#A1391;

BSA, Panreac, Barcelona, Spain) for 3 min at RT, rinsed in PBS, and incubated overnight at RT in PBS-containing 1% BSA and goat polyclonal anti-DAT (Santa Cruz Biotechnology). After incubation, the cells were rinsed in PBS and exposed to biotinylated donkey anti-goat antiserum (Jackson Immunoresearch; 1:200) followed by Cy3-conjugated streptavidin (#016−160-084; Jackson Immunorsearch; 1:1000). After further washing, the coverslips were mounted with Vectashield Mounting Medium with DAPI (#0100−20, Southernbiotech, Birmingham, AL). Control experiments in untransfected HEK cells or DAT-D_3R HEK cells in which the primary antibody was omitted were immunonegative (see supplementary Fig.1A, B). Immunofluorescence was examined under a confocal laser scanning microscopy system (RRID: SCR_0168840; Olympus FV1000, Hamburg, Germany). The intensity of DAT immunofluorescent labelling was quantified using the ImageJ program. Twelve 220 µm x 220 µm fields of 70–80 % confluent cells were randomly selected from at least two coverslips of each experimental condition from three different experiments. Images were acquired at 60X (1024 × 1024 pixels), and 3 µm x 3 µm square areas including the plasma membrane (see Fig. 3 E) of at least 10 randomly selected cells per field were analyzed. The intensity of fluorescent labeling is expressed as a percentage of fluorescence intensity in the control group.

2.7. RNA extraction and quantitative RT-PCR

Mouse substantia nigrae were dissected and homogenized using a teflon dounce homogenizer (#7984; Sigma) in PureZol reagent (#7326890; BioRad). One microgram of RNA was DNase treated and reverse transcribed using iScript reverse transcriptase (#170-8890, BioRad) according to the manufacturer's instructions. Next cDNA was used as a template for quantitative PCR SYBR dye ([95 °C, 3 min; 95 °C, 15 s; 60 °C, 30 s] x40; iQ SYBR Green Supermix 2x, #1708880EDU; Bio-Rad). Reactions were run in CFX96 Real-time Detection System (#1855196; Bio-Rad). Primer sequences were as follows: mouse DAT, forward 5′-ATCAACCCACCGCAGACACCAGT-3′, reverse 5′-GGCATCCCGGCAATAACCAT-3′; mouse TH, forward 5′-CAGCTGGAGGATGTGTCTCA-3′, reverse 5′-GGCATGACGGATGTACTGTG-3′; mouse GADPH, forward 5′-AATGTGTCCGTCGTGGATCT-3′, reverse 5′-TGTTGAAGTCGCAGGAGACA-3′. Relative expression of target genes was calculated as previously described [41].

2.8. [^{3}H]-DA uptake

This procedure was performed in striatal synaptosomes and transfected HEK cells. Synaptosomes and cell suspensions were obtained and homogenized in SBS as described for DAT expression in plasma membranes. A range of temperatures (25−35 °C), incubation times (5−30 min) and striatal protein concentrations (0.2−3 µg/µl) were checked in order to establish the working parameters in the linear ascending segment of the uptake curve. Fifty microliters of synaptosomal suspension (0.5 µg total protein/µl in striatal samples, 1 µg total protein/µl in cells) were preincubated in assay buffer with or without the selective DAT inhibitor GBR 12,935 [42] (10 µM, 30 °C, 5 min; #G9659; Sigma;). Subsequently, 20 nM [^{3}H]-DA (final concentration; #NET131250UC; PerkinElmer, Waltham, MA) was added to each tube. The total assay volume was 200 µl. After 10 min incubation at 30 °C, DA uptake was stopped by the addition of 200 µl of ice-cold assay buffer. The suspension was immediately filtered under vacuum through MultiScreen®- 0.45 µm hydrophilic filters (#MSBVN1210; Merck). The filters were washed twice with 200 µl of ice-cold assay buffer, excised and placed in scintillation vials containing 3 mL of liquid scintillation Cocktail (#L8286; Sigma), and stored overnight at RT. Accumulated radioactivity was quantified using a liquid scintillation counter (LKB Rackbeta 1214; Turku, Finland). Non-specific uptake, defined as the DA uptake in the presence of GBR 12,935, was subtracted from total uptake to define the DAT-mediated specific uptake. All assays were performed at least in triplicate.

2.9. DAT immunoprecipitation

DAT immunoprecipitation was performed both in mouse striata and DAT-D_3R HEK cells. The striata of two mice were pooled and processed as a single sample for these experiments. Tissue was homogenized in 1.5 mL ice-cold 10 mM HEPES, 0.32 M sucrose and 10 mM NEM (#E3876; Sigma) pH 7.4, and centrifuged (800 xg, 12 min, 4 °C). The supernatants were centrifuged at 22,000 xg, 15 min, 4 °C, and the resulting pellets resuspended in 100 µl M-PER. DAT-D3R HEK cells were harvested by adding cold PBS, centrifuged (1000 xg, 5 min) and resuspended in ice-cold IP buffer [20 mM HEPES pH7.6, 125 mM NaCl, glycerol 10 %, Triton X-100 1%, 1 mM EDTA, 1 mM EGTA (#E4378; Sigma), 10 mM NEM and protease-phosphatase inhibitors]. After 30 min at 4 °C of gentle shaking, the samples were centrifuged again (14,000 xg, 5 min), the pellets were discarded, and the protein concentration was quantified in the supernatants. Aliquots of 15 ug proteins of each sample were used as input controls, and 2 mg proteins were pre-cleared using Protein A/G Plus-Agarose beads (#SC2003; Santa Cruz Biotechnology) and rat IgGs (#SC3883; Santa Cruz Biotechnology) for 1 h by gentle rocking. After centrifugation, the pre-cleared supernatants were incubated with 6 µl rat monoclonal anti-DAT (Millipore) overnight at 4 °C in continuous shaking. Samples were centrifuged and incubated with new beads for 3 h. Immunocomplexes were precipitated by gentle centrifugation. After extensive washing with IP buffer, immunoprecipitates were resuspended in 40 µl Laemmli's buffer for 30 min at 37 °C, and centrifuged to collect bead-free supernatants. Samples were separated by electrophoresis in 10 % SDS-polyacrylamide gel and transferred to nitrocellulose. DAT immunoprecipitates were blotted for phosphoserine, ubiquitin, p62 and DAT using a mouse monoclonal anti-phosphoserine (#P3430; Sigma), a mouse monoclonal anti-ubiquitin (#SC8017; Santa Cruz Biotechnology; 1: 1000), a mouse monoclonal anti-p62 (#864807; R&D Systems; 1:2,000), and a goat polyclonal anti-DAT (Santa Cruz Biotechnology; 1: 5,000) or a rat polyclonal anti-DAT (Millipore; 1: 3,000). Non transfected HEK cells and cerebellum, a brain region with very low DAT expression, were used as negative controls (see supplementary Figs. 1 and 2).

2.10. In situ proximity ligation assays (PLA)

PLA allows the detection of protein interactions using oligonucleotide-conjugated antibodies, ligation of oligonucleotides by a bridging probe in a proximity-dependent manner, rolling-circle amplification, and visualization by fluorescent probes. PLA was used as a complementary technique to co-immunoprecipitation to assess the effect of PPX on DAT-p62 interaction using the Duolink II *in situ* PLA detection kit (#DUO96010; Sigma). Following Alam et al. [43] and Lopez- Cano et al. [44], striatal sections (25 µm) were placed on glass slides and HEK cells were grown and fixed as described for immunohistochemistry. They were incubated for 1 h in a preheated humidity chamber at 37 °C with the blocking solution, and overnight at 4 °C with rabbit polyclonal anti-DAT (Sigma;1:200) and mouse monoclonal anti-p62 (R&D Systems; 1: 200) antibodies in the antibody diluent. After several rinses in Buffer A [150 mM NaCl, 10 mM Tris-HCl, pH 7.4, and 0.05 % Tween20 (#P9416; Sigma)], sections were incubated (2 h, 37 °C) with PLA probes to detect rabbit and mouse antibodies (Duolink II plus PLA probe anti-rabbit, #DUO92002, and Duolink II minus PLA probe anti-mouse, #DUO92004; Sigma). Thereafter, samples were processed for ligation, amplification, and detection as described by the manufacturer. For negative controls, one of the primary antibodies was substituted by non-immune rabbit or mouse IgG, resulting in negative staining (see supplementary Fig.1B). Samples were mounted using the mounting medium with DAPI and examined under a confocal laser scanning microscopy system (Olympus). Images were acquired in Z-stack mode (10 µm total thickness, 5 z-steps). Fluorescent PLA

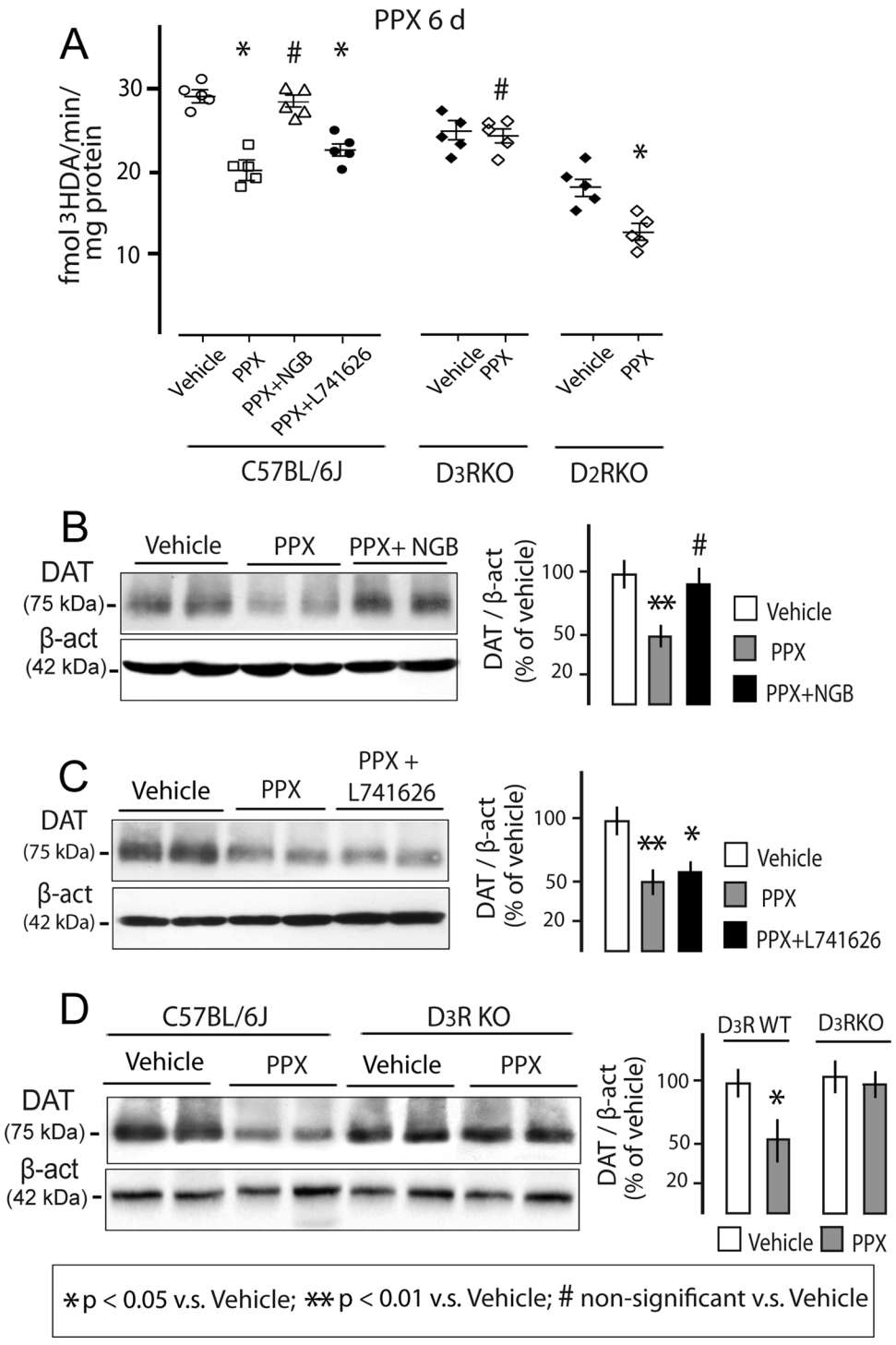

Fig. 2. DAT down-regulation induced by prolonged PPX treatment is D_3R-dependent. (A) DA uptake in the striatum of C57BL/6 J (left), D_3RKO (middle) and D_2RKO (right) mice treated with PPX (0.1 mg/kg/d, 6d). C57BL/6 J mice were also co-treated with the D_3R antagonist NGB2904 (NGB; 1 mg/kg 30 min before PPX) or the D_2R antagonist L741626 (1 mg/kg 30 min before PPX), n = 5 mice per condition. The decrease in DA uptake induced by PPX in C57BL/6 J mice ($p < 0.05$ vs. Vehicle) is reversed by co-treatment with NGB2904 ($p < 0.05$ vs. PPX; $p = 0.69$ vs. Vehicle) but not by L741626 ($p < 0.05$ vs. Vehicle). Furthermore, DA uptake is decreased in D_2RKO mice treated with PPX ($p < 0.05$ vs. Vehicle) but not in D_3RKO mice ($p = 0.54$ vs. Vehicle; Kruskal-Wallis test followed by Dunn's multiple comparison test). (B-D) Western-blot for DAT in the striatum of C57BL/6 J (B, C; n = 5 mice per condition) and D_3RKO mice (D, n = 4 mice per condition) treated with PPX (1 mg/kg/d, 6d). C57BL/6 J mice were also co-treated with NGB (B) or L741626 (C). The decrease in DAT expression induced by PPX in C57BL/6 J mice ($p < 0.05$ vs. Vehicle) is not observed in C56BL/6 J mice co-treated with NGB2904 ($p = 0.87$ vs. Vehicle) and in D_3RKO mice ($p = 0.82$ vs. Vehicle), but is maintained in C57BL/6 J mice co-treated with L741626 ($p < 0.05$ vs. Vehicle; Kruskal-Wallis test followed by Dunn's multiple comparison test). Data are presented as means ± SEM. β-act, β-actin.

point-like signals were quantified by using the ImageJ standard program. The analysis was performed in at least 24 striatal regions (100 μm x 100 μm) from 5 different mice per experimental group, and at least 20 HEK cell regions (100 μm x 100 μm) randomly selected from two coverslips of each experimental condition from three different experiments. Values are expressed as the mean number of dots ± SEM per field.

2.11. Statistics

Data were plotted using the Graph Pad Prism 5 software (RRID: SCR_002798; San Diego, CA) and presented as mean ± SEM. The statistical tests are described throughout the text in each figure legend. Briefly, the unpaired *t*-test or Mann-Whitney *U* test was performed for parametric or non-parametric analysis, respectively. Either ANOVA followed by Tukey's/Holm-Sidak multiple comparison test, or Kruskal-Wallis followed by Dunn's multiple comparison test, were performed when more than two experimental groups were compared. Data from all experiments performed were included. A level of $p < 0.05$ was considered as critical for assigning statistical significance.

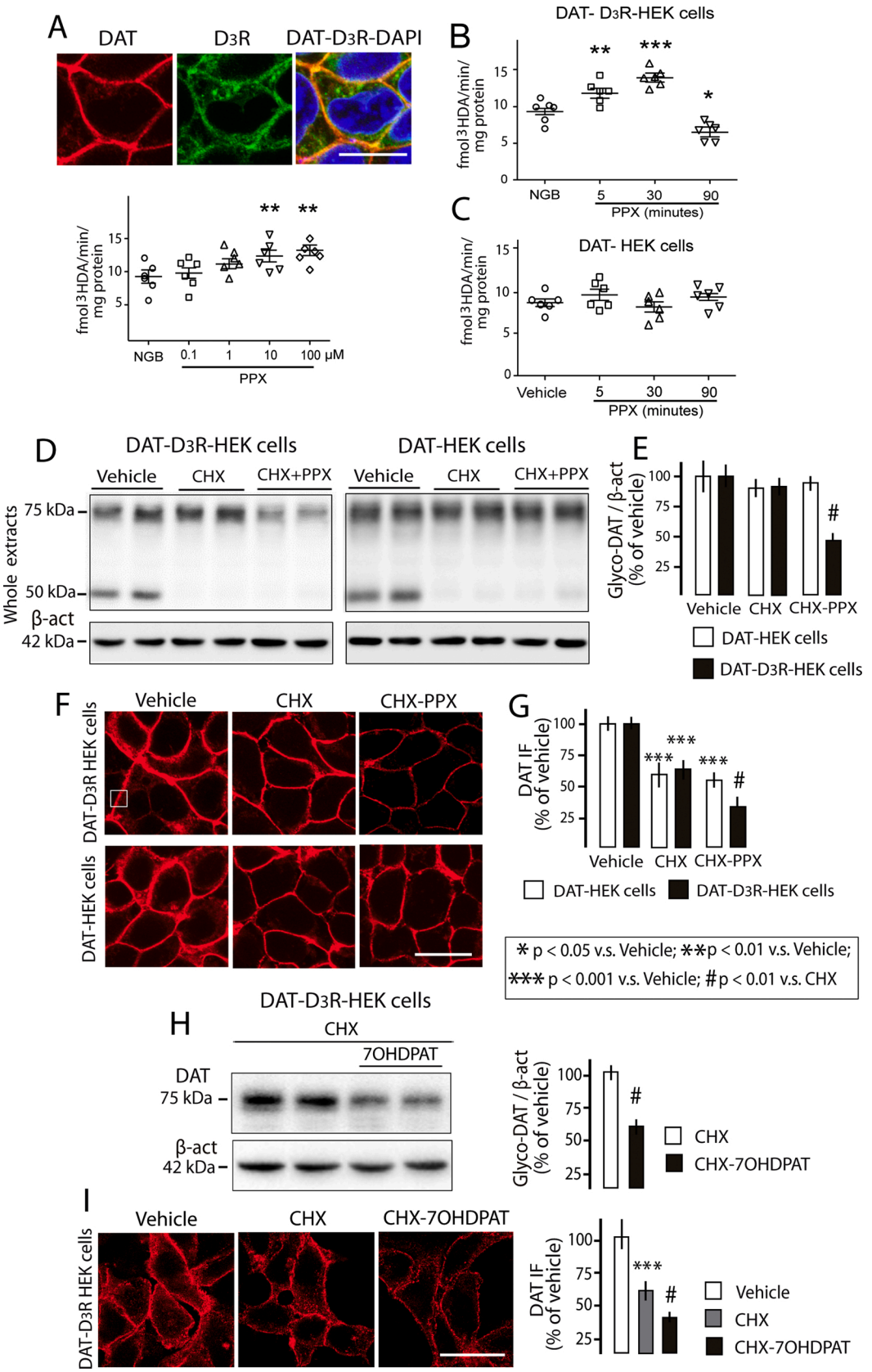

(caption on next page)

Fig. 3. DAT is down-regulated by prolonged D_3R activation in DAT-D_3R HEK cells. (A) Immunofluorescence for DAT in DAT-EGFP-D_3R transfected HEK cells and DA uptake after treatment with 0.1-100 μM PPX for 5 min. DA uptake increases after 5 min of treatment with PPX doses ≥ 10 μM ($p < 0.01$ vs. Vehicle; ANOVA followed by Dunnett's multiple comparison test; $F = 13.22$; $n = 6$ samples per experimental condition). (B, C) DA uptake in DAT-D_3R- and DAT-HEK cells treated with 10 μM PPX for 5, 30 and 90 min. Since [^{3}H]-DA signal in DAT-D_3R overexpressing cells can arise in part from the binding of the radioligand to D_3R [20], the basal [^{3}H]-DA uptake was determined by blocking D_3R with 10 μM NGB2904 (NGB). The increase in DA uptake reaches 151 % after 30 min of treatment ($p < 0.001$ vs. Vehicle) and decreases to 69 % of controls when the treatment is prolonged for 90 min ($p < 0.05$ vs. Vehicle; ANOVA followed by Dunnett's multiple comparison test; $F = 43.86$; $n = 6$ samples per experimental condition). No changes are detected in DAT-HEK cells ($p = 0.61$). (D-G) Western-blot (D, E) and immunofluorescence (F, G) for DAT in DAT-D_3R- and DA-HEK-cells treated with the protein synthesis inhibitor cycloheximide (CHX; 20μM, 45 min) and CHX + PPX (10μM, 90 min). (H, I) Western-blot and immunofluorescence for DAT in DAT-D_3R HEK cells treated with CHX and CHX+7−OH-DPAT (0.1μM, 90 min). Western-blot (D) shows that non-glycosylated (immature, 50 kDa) DAT virtually disappears after CHX treatment in both DAT-D_3R- and DAT-HEK cells (compare lanes 1 and 2 with 3 and 4). Under these conditions, the addition of PPX (D, E) or 7-OH-DPAT (H) provokes a significant decrease in the expression of glycosylated (mature, 75 kDa) DAT in DAT-D_3R cells (♯ $p < 0.01$ vs. CHX; compare lanes 3 and 4 with 5 and 6 in D (left), and lanes 1 and 2 with 3 and 4 in H) but not in DAT cells ($p = 0.24$ vs. CHX; compare lanes 3 and 4 with 5 and 6 in D, right). The intensity of labelling in DAT immunofluorescence (F, G, I) is also substantially reduced after CHX treatment in both cells. The addition of PPX (CHX + PPX) or 7-OH-DPAT (CHX + 7OHDPAT) provokes an additional labelling decrease in DAT-D_3R HEK cells but not in DAT-HEK cells. ♯ $p < 0.01$ vs. CHX; ANOVA followed by Dunnett's multiple comparison test, $F = 10.80$, $n = 6$ samples per experimental condition in E. ANOVA followed by Dunnett's multiple comparison test, $F = 42.20$, $n = 6$ samples per experimental condition in G. *t* test, $t = 7.20$, $n = 6$ samples per experimental condition in H. ANOVA followed by Dunnett's multiple comparison test, $F = 37.53$, $n = 7$ samples per experimental condition in I. Data are presented as means ± SEM. β-act, β-actin. Boxed area in F represents a square region used for the quantitative analysis of DAT immunofluorescence (see Methods section). Bar in A, F and I, 10 μm.

3. Results

3.1. Prolonged pramipexole treatment promotes a D_3R-dependent DA uptake decrease and DAT down-regulation

C57BL/6 J mice were treated with different doses (0.05–1.5 mg/kg) of the D_2R/D_3R agonist pramipexole (PPX) in two different regimens, acute (a single intraperitoneal injection and sacrifice 30 min later) and prolonged (the same treatment for six days and sacrifice on day seven). As shown in Fig. 1A, acute treatment with PPX at doses ≥ 0.1 mg/kg promotes a DA uptake increase ranging between 29–41 %. But when PPX treatment was prolonged, DA uptake decreased 23–36 % with respect to vehicle treated mice (Fig. 1B). Furthermore, as shown by western-blot (Fig. 1C, D) and immunohistochemistry (Fig. 1E, F), the striatal levels of DAT protein were significantly reduced in mice receiving ≥1 mg/kg PPX, whereas the levels of striatal tyrosine hydroxylase (TH, the dopamine limiting enzyme, and a marker of dopaminergic neurons), and nigral TH and DAT mRNAs were preserved (Fig. 1G). The finding of an increase in DA uptake in response to acute PPX treatment agrees with previous studies in rodents supporting a role of D_2 and D_3 autoreceptors in acute modulation of extracellular DA levels through DAT [15,16,45–47]. However, the results here further indicate that after 6 days of treatment with PPX doses of 0.1−1 mg/kg/d, which are human equivalent doses [48] within the therapeutic range used in Parkinson's disease (0.45–4.5 mg/d [49]), PPX causes a decrease in striatal DA uptake and DAT down-regulation.

Inasmuch as both D_2R and D_3R are expressed in presynaptic neurons, the next step was to study whether this effect is mediated by D_2R and/or D_3R. PPX also has affinity for D_4R [50], but the evidence that D_4R is not expressed in the nigrostriatal system [12] rules out its participation in this phenomenon. It should be noted that although PPX has a higher affinity for D_3R than for D_2R, its Kd for D_2R is not more than 5–7 fold higher than for D_3R [50,51]. Furthermore, D_2R expression in the mesostriatal system is about one order of magnitude higher than that of D_3R [52]. Therefore, to establish a PPX dose that is selective for one receptor or the other is highly problematic [53,54]. In order to overcome this issue, one of the receptors must be inactivated by pharmacological blockade or receptor knocking down. So, experiments were performed in C57BL/6 J mice treated with PPX and a selective D_2R or D_3R antagonist, and in D_2RKO and D_3RKO mice. As shown in Fig. 2A, the decrease in DA uptake induced by 6 days of treatment with 0.1 mg/kg/d PPX in C57BL/6 J mice was reversed by co-treatment with the selective D_3R antagonist NGB2904 (1 mg/kg i.p. 30 min before PPX) but not by co-treatment with the D_2R antagonist L741,626 (1 mg/kg s.c. 30 min before PPX). For the study of PPX effects in D_2RKO and D_3RKO mice, we first analysed the impact of D_2R and D_3R deficiency in basal DA uptake. A comparative analysis between D_2RKO and D_3RKO and their WT littermates (C57BL/6 J mice in the case of D_3RKO mice) shows that basal DA uptake is significantly lower in D_3RKO ($p < 0.01$), and in D_2RWT and D_2RKO mice ($p < 0.001$) than in C57BL/6 J mice, with no differences between D_2RWT and D_2RKO mice ($p = 0.27$; see supplementary Fig. 2A). These findings suggest differences in DA handling between the genetic background of D_2RKO and D_3RKO, and that D_3R deficiency, but not D_2R deficiency, affects basal DAT uptake. On the other hand, after prolonged PPX treatment (0.1 mg/kg/d, 6d), DA uptake was decreased in D_2RKO but not in D_3RKO mice (Fig. 2A). With respect to striatal DAT protein levels, no differences were detected between strains, and between WTs and KOs (supplementary Fig. 2B), but consistent with that found in DA uptake, the decrease in DAT expression observed after prolonged treatment with 1 mg/kg PPX in C57BL/6 J was prevented by co-treatment with NGB2904 (Fig. 2B) but not by co-treatment with L741,626 (Fig. 2C), and was not observed in D_3RKO mice (Fig. 2D). Taken together, these data indicate that the decline in DA uptake and DAT expression observed after prolonged PPX treatment is mediated by D_3R but not by D_2R.

To confirm these findings, additional experiments were performed in DAT- and DAT-D_3R-transfected HEK cells. The PPX doses having effects on DAT activity were determined by assessing [^{3}H]-DA uptake in DAT-D_3R HEK cells treated with 0.1−100 μM PPX for 5 min (Fig. 3A). Bearing in mind studies showing that [^{3}H]-DA signal in DAT-D_3R overexpressing cells can arise in part from the binding of the radioligand to D_3R [20] the specific basal [^{3}H]-DA uptake (controls) was determined by blocking D_3R with a saturating concentration of NGB2904 (10 μM) before incubation in [^{3}H]-DA. A significant increase in DA uptake (32 %, $p < 0.01$ vs. vehicle; Fig. 3A) was detected at a PPX concentration ≥10 μM. Thus, like previous studies on DAT regulation in DAT-D_2R or DAT-D_3R co-transfected cells [19,21,22], a concentration of 10 μM was used throughout the study. Consistent with that observed in mice, this dose of PPX promoted a progressive increase of DA uptake during the first 30 min, reaching 151 % of basal levels ($p < 0.001$ vs. vehicle), but after 90 min of treatment, it declined to 69 % of basal levels ($p < 0.05$ vs. vehicle; Fig. 3B). No changes were detected in cells only transfected with DAT (Fig.3C).

Following previous studies on DAT expression regulation in DAT overexpressing cells [55–57], for the study of PPX effects on DAT protein levels, DAT and DAT-D_3R transfected cells were pretreated with the protein synthesis inhibitor cycloheximide (CHX, 20 μM, 45 min, 37 °C) to avoid the contribution of newly synthesized DAT in the results. As an effect of protein synthesis blockade (CHX treatment), the immature (non-glycosylated, 50 kDa) DAT form virtually disappears in whole extracts of both DAT-D_3R- and DAT-HEK cells, without changes in the mature (glycosylated, 75 kDa) form (Fig. 3D, lanes 3 and 4; E). After adding PPX (10 μM, 90 min), a decrease of mature DAT (51 %; $p < 0.01$ vs. Vehicle) was evident in DAT-D_3R cells (Fig. 3D, left, lanes 5 and 6; E),

but not in HEK cells expressing only DAT (Fig. 3D, right, lanes 5 and 6; E). This PPX effect was also detected by immunofluorescence. CHX promoted an initial decrease of DAT immunolabelling in both DAT-D_3R and DAT cells, but PPX caused an additional immunolabelling decrease only in DAT-D_3R HEK cells (compare CHX and CHX-PPX; $p < 0.01$ vs. CHX, Fig.3F, G). Similar effects were obtained with 7-OH-DPAT, another D_2R/D_3R agonist with preferential affinity for D_3R. Following Everett and Senogles [37], 7-OH-DPAT was used at a concentration of 0.1 μM. After 90 min of treatment, 7-OH-DPAT also induced a decline of DAT expression in DAT-D_3R HEK cells pretreated with CHX ($p < 0.01$ vs. CHX; Fig. 3H, I). In sum, these findings indicate that prolonged D_3R stimulation promotes a decrease in DA uptake and DAT down-regulation.

3.2. DAT is phosphorylated and ubiquinated in response to prolonged D_3R stimulation

Previous studies indicate that DAT activity is strongly regulated by phosphorylation and ubiquitination. While phosphorylation of threonine at residue 53 in the N terminal tail has been associated to an

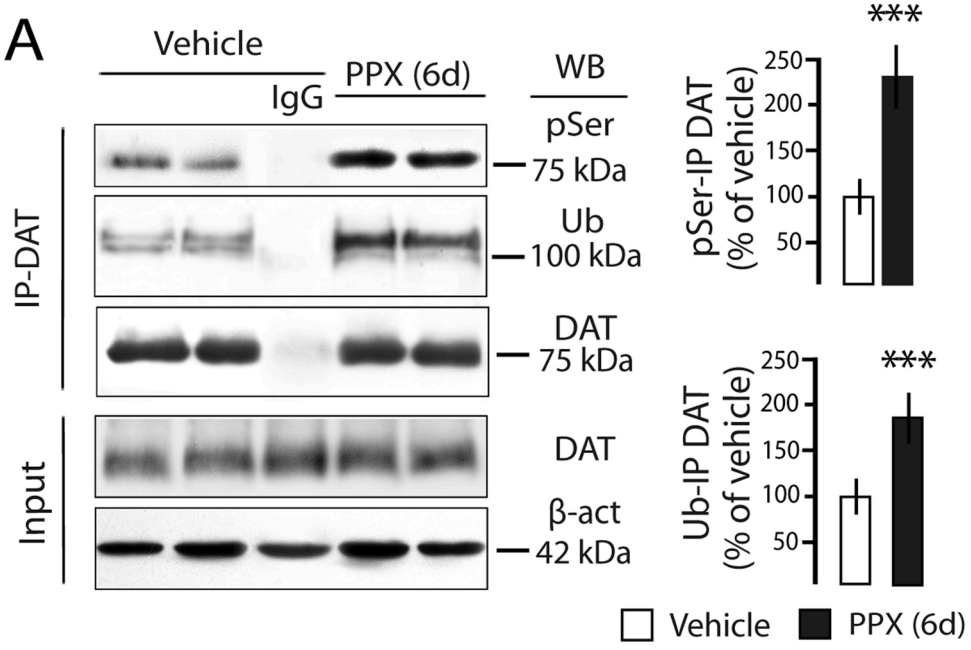

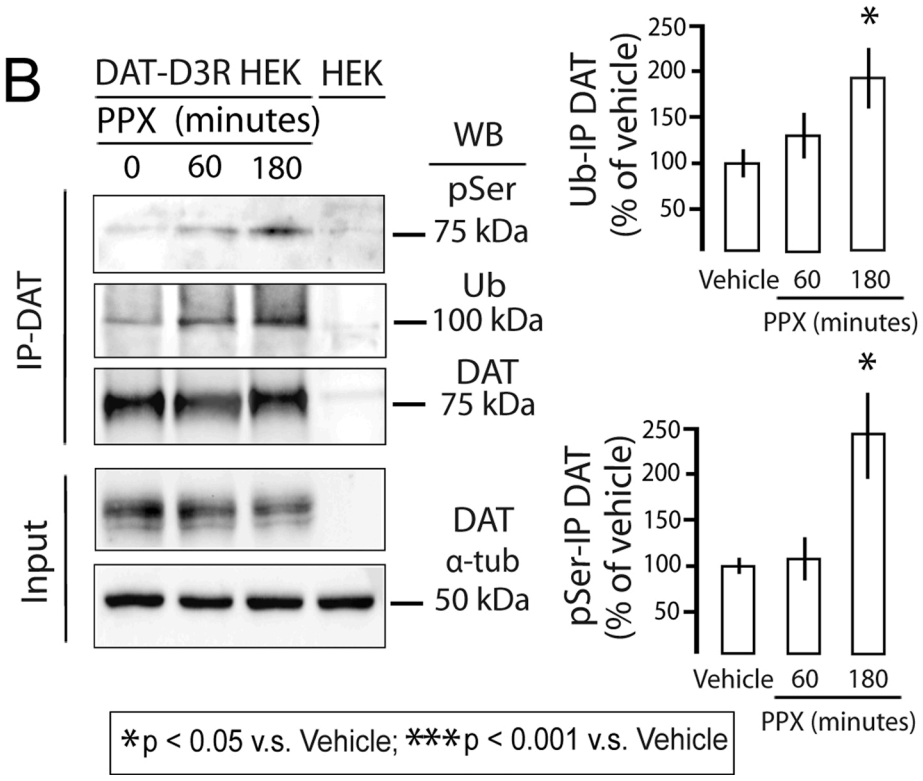

Fig. 4. Prolonged D_3R stimulation promotes DAT phosphorylation and ubiquitination. Immunoprecipitation for DAT (IP-DAT) and immunoblotting for phosphoserine (pSer), Ubiquitin (Ub) and DAT in mouse striata (A) and DAT-D_3R HEK cells (B). IgG in A refers to control immunoprecipitation using non-immune IgG. Untransfected HEK cells were used as controls (lane 4) in B. Mice were treated with 0.1 mg/kg PPX for 6 days, and cells with 10 μM PPX for 60 and 180 min. The amount of pSer and Ub immunoprecipitated with DAT increases after 6 days of PPX treatment in mice ($p < 0.001$ vs. Vehicle; Mann Whitney test; $n = 4$ independent striatal samples per experimental condition), and after 180 min of PPX treatment in HEK cells ($p < 0.05$ vs. Vehicle; Kruskal-Wallis test followed by Dunn's multiple comparison test; $n = 4$ cell culture preparations per experimental condition). Data are presented as means ± SEM. β-act, β-actin; α-tub, α-tubulin.

increase in DA transport and amphetamine-induced DA efflux [58], phosphorylation at serine residues at the distal end of the N-terminus is associated to DAT internalization and a decline in DA uptake [4]. On the other hand, ubiquitination promotes internalization and lysosomal DAT degradation [9,56,59]. The finding of a decrease in DAT activity and protein levels without changes in DATmRNA suggests that DAT may undergo phosphorylation at serine residues, ubiquitination and lysosomal degradation in response to prolonged PPX treatment. DAT phosphorylation and ubiquitination were studied using immunoprecipitation in mouse striata and DAT-D_3R HEK cells. Bearing in mind that at a dose of 1 mg/kg/d, PPX produces a significant decrease of DAT protein in whole striatal extracts of mice (Fig.1C-F), in these experiments, mice were treated with 0.1 mg/kg/d PPX, because this dose reduces DA uptake without altering total DAT protein levels. Immunoprecipitation showed that after 6 days of treatment, the relative amount of phosphorylated and ubiquitinated DAT was substantially increased in mouse striata ($p < 0.001$ vs. vehicle; Fig. 4A, lanes 4 and 5). This effect was also observed in DAT-D_3R cells. Immunoprecipitation at different times of PPX treatment revealed a significant increase in the amount of pSer and Ub immunoprecipitaed with DAT at 180 min (Fig. 4B, supplementary Fig. 2C).

The increase in DAT ubiquitination suggests that it is also internalized in response to prolonged D_3R stimulation. Consistent with the acute increase in DA uptake (see Fig.1A), the analysis of DAT protein in biotinylated membranes of striatal synaptosomes of mice receiving a single dose of 0.1 mg/kg PPX revealed a discrete but significant increase of DAT at the surface of dopaminergic terminals (Fig. 5A; $p < 0.01$ vs. vehicle). However, after six days of treatment with the same PPX dose no changes in DAT membrane levels were detected (Fig. 5A). Therefore, despite the decrease in DA uptake and the increase in DAT ubiquitination (see Fig. 1B and 4A), the absence of subcellular changes at this PPX dose, suggests that mechanisms underlying D_3R regulation of DAT in the striatum may differ depending on the agonist dose. Contrasting with mouse striata, the dynamics of DAT subcellular distribution in DAT-D_3R HEK cells closely matched DA uptake (see Fig.3B). Experiments performed in HEK cells untreated with CHX show that DAT levels increase in the plasma membrane (biotinylated fraction) during the first 30 min of PPX treatment (Fig.5B). However, after 90 min of treatment, DAT levels were decreased in the plasma membrane and increased in the cytosolic compartment (non-biotinylated fraction, Fig. 5B). In this context, it should be mentioned that during its internalization, DAT is accumulated in early and recycling endosomes when it is recycled back to the plasma membrane, or in late endosomes when it is delivered to lysosomes to be degraded [60–63]. On the other hand, p62 (sequestosome 1) is a multifunctional adaptor with an ubiquitin-associated domain that interacts with ubiquitinated cargoes on their way to lysosomes [64–66]. Furthermore, p62 is present in late endosomes and lysosomes but not in early and recycling endosomes [67,68]. So, the evidence of an interaction between DAT and p62 strengthens the idea that DAT is degraded by lysosomes in response to prolonged D_3R activation. The effect of PPX on DAT-p62 interaction was assessed using co-immunoprecipitation and PLA in DAT-D_3R HEK cells. As shown in Fig. 5C and supplementary Fig. 2C, the amount of p62 immunoprecipitated with DAT increases at 180 min of treatment ($p < 0.05$ vs. vehicle). Likewise, the number of DAT-p62 PLA dots also increased ($p < 0.01$ vs. vehicle) after 180 min of PPX treatment (Fig. 5D). In sum, the decrease in total protein levels without changes mRNA, together with its ubiquitination and interaction with p62, indicate that DAT is degraded by lysosomes in response to prolonged D_3R stimulation.

3.3. D_3R induced DAT down-regulation is PKC-dependent

It is known that protein kinase C (PKC) plays a central role in DAT phosphorylation [69] and ubiquitination [59], and that PKC-mediated ubiquitination accelerates DAT internalization and degradation [56, 57]. Therefore, PKC might also be involved in PPX-induced DAT down-regulation. This possibility was studied in DAT-D_3R HEK cells using different PKC inhibitors. As shown in Fig. 6A, the pan-PKC inhibitor bisindolylmaleimide IV (BIM; 1μM, 30 min) prevented the decrease in glycosylated DAT induced by PPX (compare lanes 7, 8 and 910) as BIM does with the direct PKC activation by phorbol myristate acetate (PMA; see lanes 3–6). Furthermore, as reflected by immunoprecipitation and PLA, BIM prevented DAT phosphorylation and ubiquitination, and DAT-p62 interaction induced by PPX (Fig. 6B, C). DAT expression was also analyzed using inhibitors more selective for conventional PKC isoforms. The decrease of glycosylated DAT was blocked by Gö6976 (15 nM, 30 min), which inhibits PKCα and PKCβI (Fig. 6D), and CGP53353 (1.5 μM, 30 min), which inhibits PKCβI and PKCβII (Fig. 6E). These data indicate that PKC, and particularly PKCβ, takes part in D_3R-mediated DAT down-regulation.

4. Discussion

The results here indicate that acute D_2R/D_3R agonist treatment promotes DAT recruitment to the plasma membrane and an increase of DA uptake, but when this treatment is prolonged, DAT is phosphorylated, ubiquitinated and degraded, with the subsequent decline of DA uptake. This effect is mediated by D_3R through a PKCβ-dependent mechanism (see Fig.7).

We know that D_2 and D_3 autoreceptors act as sensors of extracellular DA concentrations, regulating DA synthesis and release [13,70,71]. Studies in rodent striata [15–18] and using heterologous expression [19–21] show that the modulatory action of D_2 and D_3 autoreceptors on extracellular DA levels is, in part, exerted by DAT. The above studies report that DA uptake increases in response to an acute activation of D_2 and D_3 autoreceptors, although the mechanisms underlying this effect seem to be different for each receptor. D_2R expression by itself promotes DAT recruitment to the plasma membrane and physical interaction between D_2R and DAT that result in an increase of DA uptake [20]. Furthermore, its stimulation activates PKC and ERK signalling that also lead to DAT recruitment to the plasma membrane and increased DA uptake [18,19,21]. D_3R expression by itself does not affect DAT subcellular distribution and activity, but its acute stimulation activates PI3K and MAPK signalling that promotes DAT recruitment to the plasma membrane and an increase in DA uptake [22]. The findings here confirm the cooperative action of D_3R with D_2R in modulating short-time increases of extracellular DA, but also indicate that after prolonged D_3R, but not D_2R, stimulation, DAT is phosphorylated, ubiquitinated and degraded, with DA uptake decreasing below basal level. Therefore, although both receptors display a high degree of sequence homology [72], share signalling pathways [11], and probably form heterodimers [73], unlike D_2R, D_3R regulates DAT in a biphasic way.

Experiments supporting the results here were performed in DAT- and DAT-D_3R transfected HEK cells, and D_3RKO, D_2RKO and WT mice. As previously reported [74,75], basal DA uptake was not affected by D_2R delection, but it was reduced in D_3RKO mice. Data about the impact of D_3R delection on basal DAT activity differ from one study to another. Whereas Le Foll et al. [76] reported that basal DA uptake is increased in D_3RKO mice, Joyce et al. [77] found that it is reduced, and Zapata et al. [15] found no differences between WT and D_3R deficient mice. Our results agree with those by Joyce et al. [77], showing that basal DA uptake is lower in D_3RKO than in WT mice. It should be noted that D_3R has the highest affinity for DA among dopamine receptors [78], and that at a resting DA concentration of 5 nM, the estimated occupancy of D_3R is 56 % while that of D_2R is 13 % [79]. So, it is possible that in absence of D_3R, DAT becomes insensitive to small changes in extracellular DA levels, leading to the elevated levels of extracellular DA found in D_3RKO mice [80–82], but not in D_2RKO mice [74].

The decline in DA uptake and DAT protein levels in response to prolonged PPX treatment, as well as DAT phosphorylation and ubiquitination, and the D_3R-dependence of these effects were demonstrated in both HEK cells and mice. However, while the decrease in DA uptake

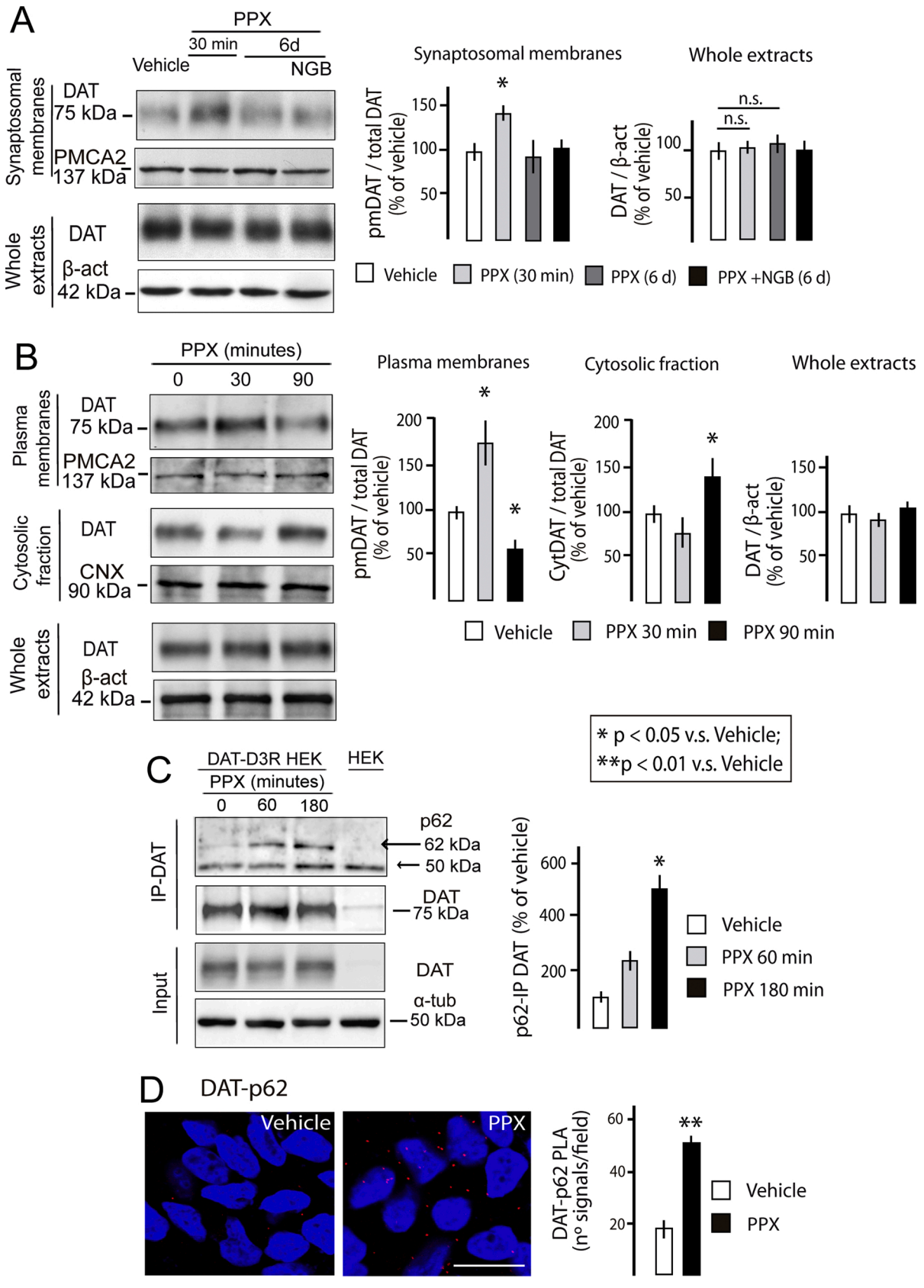

(caption on next page)

Fig. 5. D_3R activation initially promotes an increase and thereafter a decrease of DAT in the plasma membrane and accumulation in late endosomes. (A) Western-blot for DAT in the plasma membrane and whole protein extracts of mouse striatal synaptosomes of mice treated with 0.1 mg/kg PPX. Plasma membrane DAT (pmDAT) expression was normalized to plasma membrane Ca^{2+} ATPase 2 (PMCA2) and expressed as a percentage of the pmDAT/total DAT ratio in vehicle. This ratio increases 30 min after a single PPX injection ($p < 0.05$ vs. Vehicle; ANOVA followed by Dunnett's multiple comparison test, $F = 10.87$; $n = 6$ mice per condition). No changes are detected after prolonged treatment in plasma membranes and whole protein extracts. (B) Western-blot for DAT in the plasma membrane (biotyn bound, pmDAT), cytosolic fraction (biotyn unbound, CytDAT) and whole extracts of DAT-D_3R HEK cells treated with 10 μM PPX for 30 and 90 min. CytDAT was normalized to calnexin (CNX) and expressed as a percentage of the CytDAT/total DAT ratio in vehicle. Plasma membrane DAT (pmDAT) levels transiently increase at 30 min of PPX treatment ($p < 0.05$ vs. Vehicle) and thereafter (at 90 min) decrease ($p < 0.05$ vs. Vehicle), coinciding with an increase of CytDAT levels ($p < 0.05$ vs. Vehicle; ANOVA followed by Holm-Sidak's multiple comparison test; $n = 3$ independent cell cultures per experimental condition in membrane and cytosolic fractions; $n = 6$ independent cell cultures per experimental condition in whole extracts). No changes were found in whole extracts. (C) Immunoprecipitation for DAT (IP-DAT) and immunoblotting for p62 and DAT in DAT-D_3R HEK cells treated with 10 μM PPX for 60 and 180 min and in untransfected HEK cells (lane 4). The large arrow indicates 62 kDa; the small arrow indicates the heavy chain (50 kDa) of the primary antibody used for immunoprecipitation. The amount of p62 co-immunoprecipitated with DAT increases at 180 min of PPX treatment ($p < 0.05$ vs. Vehicle; ANOVA followed by Holm-Sidak's multiple comparison test; $n = 4$ independent cell cultures per experimental condition). (D) PLA for DAT and p62 in DAT-D_3R HEK cells treated with 10 μM PPX. The number of PLA signals increases after 180 min of treatment ($p < 0.01$ vs. Vehicle; Mann Whitney test; $n = 6$ independent cell samples per experimental group). Data are presented as means ± SEM. β-act, β-actin; α-tub, α-tubulin; CNX, calnexin; PMCA2, Plasma membrane Ca^{2+}ATPase. Bar in D, 10 μm.

correlated with DAT subcellular redistribution and degradation in HEK transfected cells, PPX doses <1 mg/kg/d produced a DA uptake decrease and DAT phosphorylation and ubiquitination in mouse striata, but no changes in DAT subcellular distribution and total expression. This agrees with previous data showing that, at low doses, PPX causes changes in striatal DAT proteome but not in its trafficking [23]. It should be noted that the turnover of DAT in the rodent striatum is very slow [83]. So, slight decreases in DAT expression due to an increase DAT degradation, as suggested by the evidence of DAT ubiquitination at a PPX dose of 0.1 mg/kg/d, might be not detected by Western Blot. Another possibility is that in its constitutive expression, DAT is subjected to interactions with presynaptic proteins, not evident in transfected cells, which determine dose-dependent differences in the mechanisms underlying the modulatory effect of D_3R agonists. In this respect, recent studies indicate that palmitoylation at cysteine residues exerts opposite effects to serine phosphorylation in DAT stability, and that palmitoylation and phosphorylation are reciprocally regulated [84]. So, the balance between both posttranslational modifications might underlie the decline of DAT activity without changes in its distribution. Previous studies show that single and repeated administration (4 injections in 6 h) of amphetamine and methamphetamine also cause a decrease in DA uptake without changes in the subcellular distribution and total DAT levels in rat and mouse striata [85,86]. However, in the case of repeated methamphetamine injections, total DAT levels are reduced one week after treatment [87,88]. This DAT decrease is due to the neurotoxic effect of methamphetamine as revealed by the concomitant depletion of striatal tyrosine hydroxylase (TH), the limiting enzyme in DA synthesis and a marker of dopaminergic terminals [88–90]. On the other hand, in infantile parkinsonism-dystonia associated with loss-of-function mutations of the gene encoding DAT [91,92], patients suffer a dramatic reduction of DAT which leads to dysregulation of DA synthesis and metabolism, resembling that observed in DATKO mice [93]. While extracellular levels of DA and its degradation are increased [91–93], TH expression and total levels of striatal DA are very low [93], which is the probable cause of parkinsonism in these patients. Unlike methamphetamine and DAT gene mutations, striatal levels of TH protein and midbrain levels of TH and DAT mRNAs are preserved in DAT down-regulation induced by PPX, indicating that the mesostriatal pathway is intact. This, together with the evidence of DAT phosphorylation and ubiquitination, suggests that as happens in HEK transfected cells, striatal DAT is degraded in response to prolonged D_3R stimulation.

Although diverse kinases can recognize serine and threonine residues at and near the N-terminal domain of DAT [58,94], PKC activity is nowadays regarded as a critical player in different aspects of DAT trafficking [4,57,95–97]. Interestingly, previous reports indicate that PKC is involved in D_2R-DAT interaction and D_2R-stimulated DAT recruitment to the plasma membrane [18,21], but not in the acute increase of DAT activity induced by D_3R activation [22]. The results here show that unlike the acute effect, DAT down-regulation induced by prolonged D_3R stimulation is PKC-dependent. The decrease in total DAT protein as well as its phosphorylation, ubiquitination and p62 conjugation were inhibited by the pan-PKC inhibitor BIM. Down-regulation was also inhibited by two other inhibitors, CGP53353 and Gö6976, more selective for βI and βII isoforms, supporting the participation of these conventional PKC isoforms. Despite this evidence, previous studies show that mutation of all consensus serines and threonines in DAT does not prevent its PKC-induced internalization [69]. So, it is possible that this and subsequent steps in DAT degradation may involve kinase actions on other components of the DAT multiprotein complex. DAT interactome includes presynaptic proteins such as syntaxin 1A, parkin, α-synuclein, D_2R, and the E3 ubiquitin ligase NEDD4−2 [8,9]. Using RNA interference analysis, Sorkina et al. [98] found that NEDD4−2 is essential for DAT ubiquitination and internalization, and that NEDD4−2 is activated by PKC. DAT also interacts with the tyrosine kinase Ack1, which acts as a DAT stabilizer at the plasma membrane. This interaction is broken by PKC promoting DAT endocytosis [99]. Previous studies show that DAT protein-protein interactions are modified by prolonged PPX treatment, promoting physical interaction between DAT and D_3R [23]. It should be mentioned that unlike D_2R and other GPCRs, whose internalization is associated with GPCR kinase (GRK) and β-arrestin, D_3R internalization and degradation are mediated by PKC [100,101]. Thus, different components of the DAT proteome, including D_3R itself, could also be a target of conventional PKC activation in response to prolonged D_3R stimulation.

The fact that extracellular and intracellular concentrations of DA were controlled by DAT makes DAT an interesting target for therapeutic interventions in psychiatric disorders where dopaminergic signaling is altered, and in Parkinson's disease, where, besides the decline of dopaminergic transmission, DA metabolism may contribute to cell degeneration [5,30,102]. Nowadays, DAT modulation is mostly targeted at the treatment of ADHD, stimulant abuse and depression by using direct DAT inhibitors [29,103]. Direct DAT inhibitors, such as bupropion and methylphenidate, have also been tested in Parkinson's disease patients and nonhuman primate models, but their antiparkinsonian efficacy remains uncertain [104]. The results here indicate that DA uptake may also be pharmacologically modulated through an autocrine mechanism involving the G protein-coupled D_3 autoreceptor. The involvement of G protein-coupled receptors in the regulation of Na^+ and Cl^--dependent neurotransmitter transporters was first supported by the finding of an increase in 5 H T transport following adenosine and histamine receptor activation [105,106]. Further studies have also reported NET and GAT1 redistribution from the cellular surface to the intracellular compartment in response to activation of different G protein-coupled receptors [107,108]. Here we show that besides internalization, as described for these Na^+ and Cl^--dependent neurotransmitter transporters, DAT is also ubiquitinated and degraded in response to D_3R activation.

The finding of a slower loss of mesotriatal terminals in parkinsonian

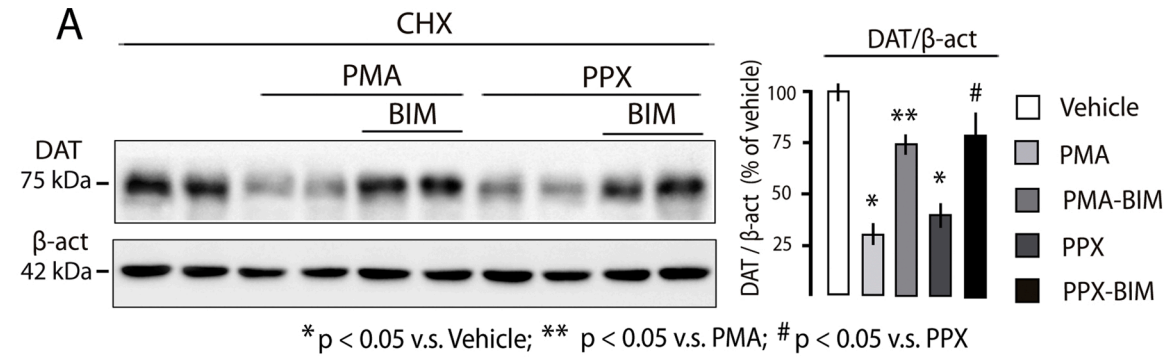

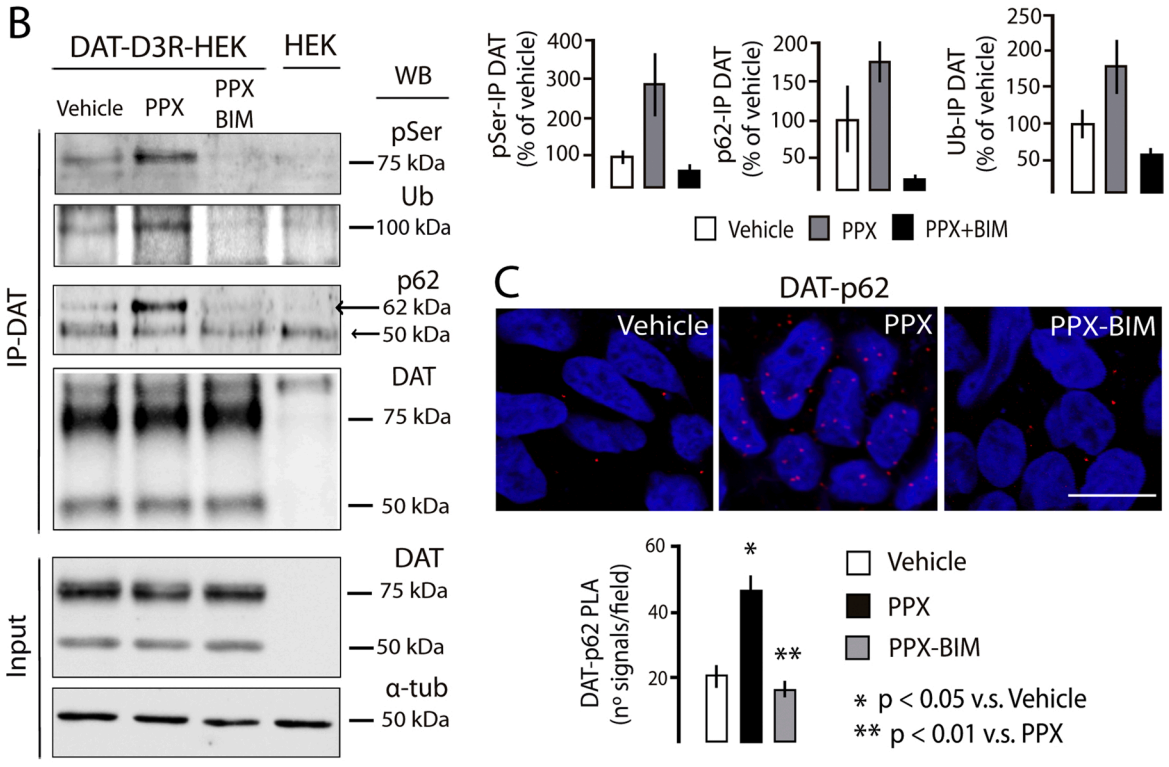

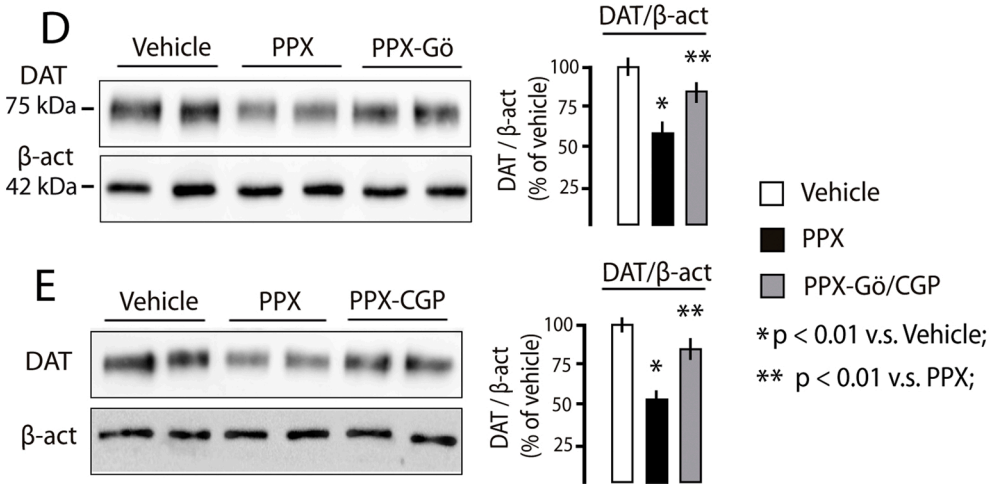

(caption on next page)

Fig. 6. DAT degradation induced by D_3R activation is PKC-dependent. (A) Western-blot for DAT in DAT-D_3R HEK cells treated with CHX (20μM, 45 min) and PPX (10 μM, 180 min). Bisindolylmaleimide IV (BIM, 1μM, 30 min before PPX) was used as PKC inhibitor, and phorbol myristate acetate (PMA, 1μM, 180 min) as positive control of PKC activation. BIM prevents the decrease in DAT expression induced by PMA (compare lanes 3 and 4 with 5 and 6) and PPX (compare lanes 7 and 8 with 9 and 10). *$p < 0.05$ vs. Vehicle, **$p < 0.05$ vs. PMA, ♯ $p < 0.05$ vs. PPX; Kruskal-Wallis test followed by Dunn's multiple comparison test; $n = 6$ independent cell samples per experimental group. (B) Immunoprecipitation for DAT (IP-DAT) and Western-blotting for phosphoserine (pSer), ubiquitin (Ub), p62 (p62) and DAT (DAT) in DAT-D_3R HEK cells. BIM (BIM-PPX) prevents DAT phosphorylation and ubiquitination, and DAT-p62 interaction induced by PPX ($n = 3$ independent cell cultures per experimental condition). (C) PLA for DAT and p62 in DAT-D_3R HEK cells. The increase in the PLA signal number induced by PPX is blocked by BIM (PPX-BIM). * $p < 0.05$ vs. Vehicle, ** $p < 0.01$ vs. PPX; Kruskal-Wallis test followed by Dunn's multiple comparison test; $n = 6$ independent cell samples per experimental group. (D, E) Western-blot for DAT in DAT-D_3R HEK cells treated with CHX (vehicle), CHX and PPX (PPX) and CHX, PPX and two conventional PKC inhibitors, Gö6976 (PPX-Gö, D) and CGP53353 (PPX-CGP, E). The decrease in DAT expression induced by PPX ($p < 0.01$ vs. Vehicle) was reversed by both PKC inhibitors ($p < 0.01$ vs. PPX; Kruskal-Wallis test followed by Dunn's multiple comparison test; $n = 5$; 2-3 independent cell cultures per experimental condition from 2 different experiments). Data are presented as means ± SEM. β-act, β-actin; α-tub, α-tubulin. Bar in C, 10 μm.

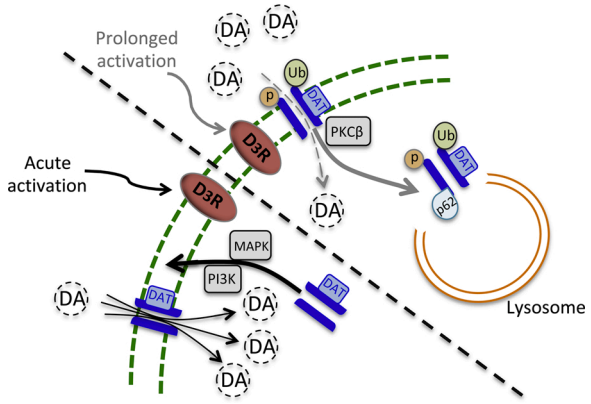

Fig. 7. A diagram showing the putative mechanisms underlying the effects of acute and prolonged D_3R activation on DAT. Acute activation of D_3R (left side) promotes DAT recruitment to the plasma membrane (thick black arrow) and an increase in DA uptake (solid thin black arrows). This effect is MAPK- and PI3K-dependent [22]. After prolonged activation (right side), DAT is phosphorylated (p), ubiquitinated (Ub) and internalized (thick gray arrow), leading to a decrease in DA uptake (dashed thin gray arrow). Internalized DAT interacts with p62 at late endosomes and lysosomes to be degraded. DAT downregulation is PKCβ-dependent.

patients treated with PPX or ropinirole in comparison with those treated with L-dopa has suggested that D_2R/D_3R agonists have neuroprotective effects on dopaminergic neurons [24,25]. This idea is also supported by experimental reports showing that treatment with D_2R/D_3R agonists reduces the cell loss induced by neurotoxins [26,109]. Further studies report that D_2R/D_3R agonist neuroprotection is associated with D_3R rather than D_2R actions [24–26110,111], and that D_2R-DAT interaction can even contribute to the vulnerability of DA cells. For example, neurotoxic effects of methamphetamine and MDMA on dopaminergic neurons are reduced by genetic inactivation of D_2R in mice [34] or pharmacological blockade in rats [85], and disruption of D_2R-DAT interaction prevents the neurotoxic effect of dopamine in SH-SY5Y cells [112]. Thus, the increase in cytosolic DA resulting from the interaction between D_2R and DAT may contribute to dopaminergic cell vulnerability. Conversely, as the results here show, prolonged D_3R stimulation may have a neuroprotective effect by reducing cytosolic levels of DA through its inhibitory effect on DAT. On the other hand, based on the dopamine hypothesis of bipolar and major depressive disorders [5,30], D_2R/D_3R agonists have been assayed as adjunctive treatment in depression [29,103]. There are data suggesting that PPX reduces depressive symptoms and increases the rate of clinical remissions [27,28]. The results here indicate that presynaptic D_3R-DAT interaction can also potentiate striatal dopaminergic transmission and account for the antidepressant effect of D_3R agonists.

In sum, prolonged activation of D_3 autoreceptors promotes phosphorylation, ubiquitination and degradation of DAT through a PKCβ-dependent mechanism. This effect offers an alternative to DAT inhibitors in DA uptake modulation, and can underlie the neuroprotective and antidepressant actions reported for some D_2R/D_3R agonists in Parkinson's disease and bipolar depression, respectively. In contrast to D_3, D_2 autoreceptors may reinforce DAT activity, contributing to the vulnerability of dopaminergic cells to dopamine and recreational drugs. Differences between D_2R and D_3R on DAT regulation highlight the need for the design of D_3R-selective agonists. Although some moderately selective D_3R agonists have been identified, the high sequence homology between D_2R and D_3R [87] is still a major obstacle in this challenge. An additional complication arises from the fact that GPCRs can act through G protein-dependent and G protein-independent pathways, each of which recruits different downstream signaling molecules resulting in different functional effects [113,114]. Although physiological functions of DA require the integrity of both pathways [115], overactivation of multiple pathways under pathological conditions can lead to adverse effects [116]. The search for receptor- and pathway-selective ligands shows that some D_3R agonists have biased signaling through the G-protein dependent pathway and efficacy against L-dopa induced dyskinesia in animal models of Parkinson's disease [117]. Advances in structural biology and the use of high-throughput screening will help towards finding more D_3R selective agonists efficient in DAT modulation.

Author contributions

DLR and TGH conceived and designed the study. DLR, FFR, PBC, JCH, DAO, AFC, ICM, JSH, VMI and JRN performed the experiments. DLR, FFR and TGH analyzed the data. DLR and TGH wrote the paper.

Declaration of Competing Interest

The authors report no declarations of interest.

Acknowledgements

This work was supported by the Spanish Ministerio de Economía y Competitividad [BFU2016-77363-R; PID2019-105795RB-I00] and the Gobierno Autónomo de Canarias [2018-00000034] to TGH. DLR was supported by the "Programa Agustín de Betancourt" (Cabildo Insular de Tenerife). FFR and AFC were supported by the program "Ayudas para contratos predoctorales para la formación de doctores", the Spanish Ministerio de Economía y Competitividad [BES-2014-067781 and BES-2017-079923, respectively], and VMI by the program "Ayudas para la formación de personal investigador dentro de programas de doctorado en Canarias" [TESIS2018010044].

Appendix A. Supplementary data

Supplementary material related to this article can be found, in the online version, at doi:https://doi.org/10.1016/j.phrs.2021.105434.

References

[1] J.A. Girault, P. Greengard, The neurobiology of dopamine signaling, Arch. Neurol. 61 (2004) 641–644, https://doi.org/10.1001/archneur.61.5.641.

[2] O. Hornykiewicz, Basic research on dopamine in Parkinson's disease and the discovery of the nigrostriatal dopamine pathway: the view of an eyewitness, Neurodegener. Dis. 5 (2008) 114–117, https://doi.org/10.1159/000113678.

[3] B. Giros, M. Jaber, S.R. Jones, R.M. Wightman, M.G. Caron, Hyperlocomotion and indifference to cocaine and amphetamine in mice lacking the dopamine transporter, Nature 379 (1996) 606–612, https://doi.org/10.1038/379606a0.

[4] R.A. Vaughan, J.D. Foster, Mechanisms of dopamine transporter regulation in normal and disease states, Trends Pharmacol. Sci. 34 (2013) 489–496, https://doi.org/10.1016/j.tips.2013.07.005.

[5] A.H. Ashok, T.R. Marques, S. Jauhar, M.M. Nour, G.M. Goodwin, A.H. Young, O. D. Howes, The dopamine hypothesis of bipolar affective disorder: the state of art and implications for treatment, Mol. Psychiatry 22 (2017) 666–679, https://doi.org/10.1038/mp.2017.16.

[6] U. Gether, P.H. Andersen, O.M. Larsson, A. Schousboe, Neurotransmitter transporters: molecular function of important drug targets, Trends Pharmacol. Sci. 27 (2006) 375–383, https://doi.org/10.1016/j.tips.2006.05.003.

[7] O.V. Mortensen, S.G. Amara, Dynamic regulation of the dopamine transporter, Eur. J. Pharmacol. 479 (2003) 159–170, https://doi.org/10.1016/j.ejphar.2003.08.066.

[8] G.E. Torres, The dopamine transporter proteome, J. Neurochem. 97 (Suppl 1) (2006) 3–10, https://doi.org/10.1111/j.1471-4159.2006.03719.x, 2006.

[9] J. Eriksen, T.N. Jørgensen, U. Gether, Regulation of dopamine transporter function by protein-protein interactions: new discoveries and methodological challenges, J. Neurochem. 113 (2010) 27–41, https://doi.org/10.1111/j.1471-4159.2010.06599.x.

[10] C. Missale, S.R. Nash, S.W. Robinson, M. Jaber, M.G. Caron, Dopamine receptors: from structure to function, Physiol. Rev. 78 (1998) 189–225, https://doi.org/10.1152/physrev.1998.78.1.189.

[11] J.M. Beaulieu, R.R. Gainetdinov, The physiology, signaling, and pharmacology of dopamine receptors, Pharmacol. Rev. 63 (2011) 182–217, https://doi.org/10.1124/pr.110.002642.

[12] D. Noain, M.E. Avale, C. Wedemeyer, D. Calvo, M. Peper, M. Rubinstein, Identification of brain neurons expressing the dopamine D4 receptor gene using BAC transgenic mice, Eur. J. Neurosci. 24 (2016) 2429–2438, https://doi.org/10.1111/j.1460-9568.2006.05148.x.

[13] P. Sokoloff, J. Diaz, B. Le Foll, O. Guillin, L. Leriche, E. Bezard, C. Gross, The dopamine D3 receptor: a therapeutic target for the treatment of neuropsychiatric disorders, CNS Neurol. Disord. Drug Targets 5 (2006) 25–43, https://doi.org/10.2174/187152706784111551.

[14] C.P. Ford, The role of D2-autoreceptors in regulating dopamine neuron activity and transmission, Neuroscience 282 (2014) 13–22, https://doi.org/10.1016/j.neuroscience.2014.01.025.

[15] A. Zapata, J.M. Witkin, T.S. Shippenberg, Selective D3 receptor agonist effects of (+)-PD128907 on dialysate dopamine at low doses, Neuropharmacology 41 (2001) 351–359, https://doi.org/10.1016/s0028-3908(01)00069-7.

[16] A. Zapata, T.S. Shippenberg, D(3) receptor ligands modulate extracellular dopamine clearance in the nucleus accumbens, J. Neurochem. 81 (2002) 1035–1042, https://doi.org/10.1046/j.1471-4159.2002.00893.x.

[17] M. Benoit-Marand, B. Ballion, E. Borrelli, T. Boraud, F. Gonon, Inhibition of dopamine uptake by D2 antagonists: an in vivo study, J. Neurochem. 116 (2011) 449–458, https://doi.org/10.1111/j.1471-4159.2010.07125.x.

[18] A.G. Zestos, C. Carpenter, Y. Kim, M.J. Low, R.T. Kennedy, M.E. Gnegy, Ruboxistaurin reduces cocaine-stimulated increases in extracellular dopamine by modifying dopamine autoreceptor activity, ACS Chem. Neurosci. 10 (2019) 1960–1969, https://doi.org/10.1021/acschemneuro.8b00259.

[19] E.A. Bolan, B. Kivell, V. Jaligam, M. Oz, L.D. Jayanthi, Han Y, N. Sen, E. Urizar, I. Gomes, L.A. Devi, S. Ramamoorthy, J.A. Javitch, A. Zapata, T.S. Shippenberg, D2 receptors regulate dopamine transporter function via an extracellular signal-regulated kinase 1 and 2-dependent and phosphoinositide 3 kinase-independent mechanism, Mol. Pharmacol. 71 (2007) 1222–1232, https://doi.org/10.1124/mol.106.027763.

[20] F.J. Lee, L. Pei, A. Moszczynska, B. Vukusic, P.J. Fletcher, F. Liu, Dopamine transporter cell surface localization facilitated by a direct interaction with the dopamine D2 receptor, EMBO J. 26 (2007) 2127–2136, https://doi.org/10.1038/sj.emboj.7601656.

[21] R. Chen, C.P. Daining, H. Sun, R. Fraser, S.L. Stokes, M. Leitges, M.E. Gnegy, Protein kinase Cβ is a modulator of the dopamine D2 autoreceptor-activated trafficking of the dopamine transporter, J. Neurochem. 125 (2013) 663–672, https://doi.org/10.1111/jnc.12229.

[22] A. Zapata, B. Kivell, Y. Han, J.A. Javitch, E.A. Bolan, D. Kuraguntla, V. Jaligam, M. Oz, L.D. Jayanthi, D.J. Samuvel, S. Ramamoorthy, T.S. Shippenberg, Regulation of dopamine transporter function and cell surface expression by D3 dopamine receptors, J. Biol. Chem. 282 (2007) 35842–35854, https://doi.org/10.1074/jbc.M611758200.

[23] J. Castro-Hernandez, D. Afonso-Oramas, I. Cruz-Muros, J. Salas-Hernandez, P. Barroso-Chinea, R. Moratalla, M.J. Millan, T. Gonzalez-Hernandez, Prolonged treatment with pramipexole promotes physical interaction of striatal dopamine D3 autoreceptors with dopamine transporters to reduce dopamine uptake, Neurobiol. Dis. 74 (2015) 323–335, https://doi.org/10.1016/j.nbd.2014.12.007.

[24] Parkinson Study Group, Dopamine transporter brain imaging to assess the effects of pramipexole vs levodopa on Parkinson disease progression, JAMA 287 (2002) 1653–1661, https://doi.org/10.1001/jama.287.13.1653.

[25] A.L. Whone, R.L. Watts, A.J. Stoessl, M. Davis, S. Reske, C. Nahmias, A.E. Lang, O. Rascol, M.J. Ribeiro, P. Remy, W.H. Poewe, R.A. Hauser, D.J. Brooks, Slower progression of Parkinson's disease with ropinirole versus levodopa: the REAL-PET study, Ann. Neurol. 54 (2003) 93–101, https://doi.org/10.1002/ana.10609.

[26] J.N. Joyce, M.J. Millan, Dopamine D3 receptor agonists for protection and repair in Parkinson's disease, Curr. Opin. Pharmacol. 7 (2007) 100–105, https://doi.org/10.1016/j.coph.2006.11.004.

[27] C.A. Zarate Jr, J.L. Payne, J. Singh, J.A. Quiroz, D.A. Luckenbaugh, K.D. Denicoff, D.S. Charney, H.K. Manji, Pramipexole for bipolar II depression: a placebo-controlled proof of concept study, Biol. Psychiatry 56 (2004) 54–60, https://doi.org/10.1016/j.biopsych.2004.03.013.

[28] C. Cusin, N. Iovieno, D.V. Iosifescu, A.A. Nierenberg, M. Fava, A.J. Rush, R. H. Perlis, A randomized, double-blind, placebo-controlled trial of pramipexole augmentation in treatment-resistant major depressive disorder, J. Clin. Psychiatry 74 (2013) e636–641, https://doi.org/10.4088/JCP.12m08093.

[29] B. Dell'Osso, T.A. Ketter, L. Cremaschi, G. Spagnolin, A.C. Altamura, Assessing the roles of stimulants/stimulant-like drugs and dopamine agonists in the treatment of bipolar depression, Curr. Psychiatry Rep. 15 (2013) 378, https://doi.org/10.1007/s11920-013-0378-z.

[30] P. Belujon, A.A. Grace, Dopamine system dysregulation in major depressive disorders, Int. J. Neuropsychopharmacol. 20 (2017) 1036–1046, https://doi.org/10.1093/ijnp/pyx056.

[31] D. Accili, C.S. Fishburn, J. Drago, H. Steiner, J.E. Lachowicz, B.H. Park, E. B. Gauda, E.J. Lee, M.H. Cool, D.R. Sibley, C.R. Gerfen, H. Westphal, S. Fuchs, A targeted mutation on the D3 dopamine receptor gene is associated with hyperactivity in mice, Proc. Natl. Acad. Sci. U.S.A. 93 (1996) 1945–1949, https://doi.org/10.1073/pnas.93.5.1945.

[32] G. Collo, F. Bono, L. Cavalleri, L. Plebani, E. Merlo Pich, M.J. Millan, P.F. Spano, C. Missale, Pre-synaptic dopamine D (3) receptor mediates cocaine-induced structural plasticity in mesencephalic dopaminergic neurons via ERK and Akt pathways, J. Neurochem. 120 (2012) 765–778, https://doi.org/10.1111/j.1471-4159.2011.07618.x.

[33] M.A. Kelly, M. Rubinstein, S.L. Asa, G. Zhang, C. Saez, J.R. Bunzow, R.G. Allen, R. Hnasko, N. Ben-Jonathan, D.K. Grandy, M.J. Low, Pituitary lactotroph hyperplasia and chronic hyperprolactinemia in dopamine D2 receptor-deficient mice, Neuron 19 (1997) 103–113, https://doi.org/10.1016/s0896-6273(00)80351-7.

[34] N. Granado, S. Ares-Santos, I. Oliva, E. O'Shea, E.D. Martin, M.I. Colado, R. Moratalla, Dopamine D2-receptor knockout mice are protected against dopaminergic neurotoxicity induced by methamphetamine or MDMA, Neurobiol. Dis. 42 (2011) 391–403, https://doi.org/10.1016/j.nbd.2011.01.033.

[35] D. Afonso-Oramas, I. Cruz-Muros, D. Alvarez de la Rosa, P. Abreu, T. Giraldez, J. Castro-Hernandez, J. Salas-Hernandez, J.L. Lanciego, M. Rodriguez, T. Gonzalez-Hernandez, Dopamine transporter glycosylation correlates with the vulnerability of midbrain dopaminergic cells in Parkinson's disease, Neurobiol. Dis. 36 (2009) 494–508, https://doi.org/10.1016/j.nbd.2009.09.002.

[36] A.M. Gonzalez, D.R. Sibley, [3H]-7-OH-DPAT is capable of labeling D2 as well as D3 receptors, Eur. J. Pharmacol. 272 (1995) R1–R3, https://doi.org/10.1016/0014-2999(94)00738-s.

[37] P.B. Everett, S.E. Senogles, D3 dopamine receptor activates phospholipase D through a pertussis toxin-insensitive pathway, Neurosci. Lett. 371 (2004) 34–39, https://doi.org/10.1016/j.neulet.2004.08.033.

[38] I. Cruz-Muros, D. Afonso-Oramas, P. Abreu, M.M. Pérez-Delgado, M. Rodríguez, T. González-Hernández, Aging effects on the dopamine transporter expression and compensatory mechanisms, Neurobiol Aging.30 (2009) 973–986, https://doi.org/10.1016/j.neurobiolaging.2007.09.009.

[39] P. Barroso-Chinea, I. Cruz-Muros, D. Afonso-Oramas, J. Castro-Hernández, J. Salas-Hernández, A. Chtarto, D. Luis-Ravelo, M. Humbert-Claude, L. Tenenbaum, T. González-Hernández, Long-term controlled GDNF over-expression reduces dopamine transporter activity without affecting tyrosine hydroxylase expression in the rat mesostriatal system, Neurobiol. Dis. 88 (2016) 44–54, https://doi.org/10.1016/j.nbd.2016.01.002.

[40] T. Gonzalez-Hernandez, P. Barroso-Chinea, M. Rodríguez, Response of the GABAergic and dopaminergic mesostriatal projections to the lesion of the contralateral dopaminergic mesostriatal pathway in the rat, Mov. Disord. 19 (2004) 1029–1042, https://doi.org/10.1002/mds.20206.

[41] M.W. Pfaffl, A new mathematical model for relative quantification in real-time RT–PCR, Nucleic Acids Res. 29 (2001) e45, https://doi.org/10.1093/nar/29.9.e45.

[42] M.E. Reith, L.L. Coffey, C. Xu, N.H. Chen, GBR 12909 and 12935 block dopamine uptake into brain synaptic vesicles as well as nerve endings, Eur. J. Pharmacol. 253 (1994) 175–178, https://doi.org/10.1016/0014-2999(94)90774-9.

[43] M.S. Alam, Proximity ligation assay (PLA), Curr. Protoc. Immunol. 123 (2009) e58, https://doi.org/10.1002/cpim.58.

[44] M. Lopez-Cano, V. Fernandez-Dueñas, F. Ciruela, Proximiy ligation assay image analysis protocol: addressing receptor-receptor interactions, Methods Mol. Biol. 2040 (2019) 41–50, https://doi.org/10.1007/978-1-4939-9686-5_3.

[45] S.M. Meiergerd, T.A. Patterson, J.O. Schenk, D2 receptors may modulate the function of the transporter for dopamine: kinetic evidence from studies in vitro and in vivo, J. Neurochem. 61 (1993) 764–767, https://doi.org/10.1111/j.1471-4159.1993.tb02185.x.

[46] W.A. Cass, G.A. Gerhardt, Direct in vivo evidence that D2 dopamine receptors can modulate dopamine uptake, Neurosci. Lett. 176 (1994) 259–263, https://doi.org/10.1016/0304-3940(94)90096-5.

[47] A. Zapata, T.S. Shippenberg, Lack of functional D2 receptors prevents the effects of the D3-preferring agonist (+)-PD 128907 on dialysate dopamine levels,

Neuropharmacology 48 (2005) 43–50, https://doi.org/10.1016/j.neuropharm.2004.09.003.
[48] A. Nair, M.A. Morsy, S. Jacob, Dose translation between laboratory animals and human in preclinical and clinical phase of drug development, Drug Dev. Res. (October 21) (2018), https://doi.org/10.1002/ddr.21461.
[49] K.M. Shannon, J.P. Bennett Jr, J.H. Friedman, Efficacy of pramipexole, a novel dopamine agonist, as monotherapy in mild and moderate Parkinson's disease. The Pramipexole Study Group, Neurology 49 (1997) 1580–1587, https://doi.org/10.1212/wnl.49.3.724.
[50] J. Mierau, F.J. Schneider, H.A. Ensinger, C.L. Chio, M.E. Lajiness, R.M. Huff, Pramipexole binding and activation of cloned and expressed dopamine D2, D3 and D4 receptors, Eur. J. Pharmacol. 290 (1995) 29–36, https://doi.org/10.1016/0922-4106(95)90013-6.
[51] M.F. Piercey, W.E. Hoffmann, M.W. Smith, D.K. Hyslop, Inhibition of dopamine neuron firing by pramipexole, a dopamine D3 receptor-preferring agonist: comparison to other dopamine receptor agonists, Eur. J. Pharmacol. 312 (1996) 35–44, https://doi.org/10.1016/0014-2999(96)00454-2.
[52] N.M. Richtand, J.R. Kelsoe, D.S. Segal, R. Kuczenski, Regional quantification of D1, D2, and D3 dopamine receptor mRNA in rat brain using a ribonuclease protection assay, Brain Res. Mol. Brain Res. 33 (1995) 97–103, https://doi.org/10.1016/0169-328x(95)00112-6.
[53] K.D. Burris, M.A. Pacheco, T.M. Filtz, M.P. Kung, H.F. Kung, P.B. Molinoff, Lack of discrimination by agonists for D2 and D3 dopamine receptors, Neuropsychopharmacology 12 (1995) 335–345, https://doi.org/10.1016/0893-133X(94)00099-L.
[54] K.A. Neve, C.J. DuRand, M.M. Teeter, Structural analysis of the mammalian D2, D3, and D4 dopamine receptors, in: A. Sidhu, M. Laruelle, P. Vernier (Eds.), Dopamine Receptors and Transporters, Taylor and Francis, Boca Raton, 2003, pp. 71–128. ISBN-13: 978-0824708542.
[55] C. Saunders, J.V. Ferrer, L. Shi, J. Chen, G. Merrill, M.E. Lamb, L.M. Leeb-Lundberg, L. Carvelli, J.A. Javitch, A. Galli, Amphetamine-induced loss of human dopamine transporter activity: an internalization-dependent and cocaine-sensitive mechanism, Proc. Natl. Acad. Sci. U.S.A. 97 (2000) 6850–6855, https://doi.org/10.1073/pnas.110035297.
[56] M. Miranda, C.C. Wu, T. Sorkina, D.R. Korstjens, A. Sorkin, Enhanced ubiquitylation and accelerated degradation of the dopamine transporter mediated by protein kinase C. J, Biol. Chem. 280 (2005) 35617–35624, https://doi.org/10.1074/jbc.M506618200.
[57] W.C. Hong, S.G. Amara, Differential targeting of the dopamine transporter to recycling or degradative pathways during amphetamine- or PKC-regulated endocytosis in dopamine neurons, FASEB J. 27 (2013) 2995–3007, https://doi.org/10.1096/fj.12-218727.
[58] J.D. Foster, J.W. Yang, A.E. Moritz, S. Challasivakanaka, M.A. Smith, M. Holy, K. Wilebski, H.H. Sitte, R.A. Vaughan, Dopamine transporter phosphorylation site threonine 53 regulates substrate reuptake and amphetamine-stimulated efflux, J. Biol. Chem. 287 (2012) 29702–29712, https://doi.org/10.1074/jbc.M112.367706.
[59] M. Miranda, K.R. Dionne, T. Sorkin, A. Sorkin, Three ubiquitin conjugation sites in the amino terminus of the dopamine transporter mediate protein kinase C-dependent endocytosis of the transporter, Mol. Biol. Cell 18 (2007) 313–323, https://doi.org/10.1091/mbc.e06-08-0704.
[60] M.K. Loder, H.E. Melikian, The dopamine transporter constitutively internalizes and recycles in a protein kinase C-regulated manner in stably transfected PC12 cell lines, J. Biol. Chem. 278 (2003) 22168–22174, https://doi.org/10.1074/jbc.M301845200.
[61] T. Sorkin, B.R. Hoover, N.R. Zahniser, A. Sorkin, Constitutive and protein kinase C-induced internalization of the dopamine transporter is mediated by a clathrin-dependent mechanism, Traffic 6 (2005) 157–170, https://doi.org/10.1111/j.1600-0854.2005.00259.x.
[62] J. Eriksen, S.G. Rasmussen, T.N. Rasmussen, C.B. Vaegter, J.H. Cha, M.F. Zou, A. H. Newman, U. Gether, Visualization of dopamine transporter trafficking in live neurons by use of fluorescent cocaine analogs, J. Neurosci. 29 (2009) 6794–6808, https://doi.org/10.1523/JNEUROSCI.4177-08.2009.
[63] A. Rao, D. Simmons, A. Sorkin, Differential subcellular distribution of endosomal compartments and the dopamine transporter in dopaminergic neurons, Mol. Cell. Neurosci. 46 (2011) 148–158, https://doi.org/10.1016/j.mcn.2010.08.016.
[64] M.L. Sheibenhener, T. Geetha, M.W. Wooten, Sequestosome 1/p62–more than just a scaffold, FEBS Lett. 581 (2007) 175–179, https://doi.org/10.1016/j.febslet.2006.12.027.
[65] W.J. Liu, L. Ye, W.F. Huang, L.J. Guo, Z.G. Xu, H.L. Wu, C. Yang, H.F. Liu, p62 links the autophagy pathway and the ubiquitin-proteasoe system upon ubiquitinated protein degradation, Cell. Mol. Biol. Lett. 21 (2016) 29, https://doi.org/10.1186/s11658-016-0031-z.
[66] P. Sanchez-Martin, M. Komatsu, p62/SQSTM1: steering the cell through health and disease, J. Cell. Sci. 131 (2018), https://doi.org/10.1242/jcs.222836 pii: jcs222836.
[67] P. Sanchez, G. De Carcer, I.V. Sandoval, J. Moscat, M.T. Diaz-Meco, Localization of atypical protein kinase C isoforms into lysosome-targeted endosomes through interaction with p62, Mol. Cell. Biol. 18 (1998) 3069–3080, https://doi.org/10.1128/mcb.18.5.3069.
[68] A. Meenhuis, P.A. van Veelen, H. de Looper, N. van Boxtel, I.J. van den Berge, S. M. Sun, E. Taskesen, P. Stern, A.H. de Ru, A.J. van Adrichem, J. Demmers, M. Jongen-Lavrencic, B. Löwenberg, I.P. Touw, P.A. Sharp, S.J. Erkeland, MiR-17/20/93/106 promote hematopoietic cell expansion by targeting sequestosome 1-regulated pathways in mice, Blood 118 (2011) 916–925, https://doi.org/10.1182/blood-2011-02-336487.
[69] C. Granas, J. Ferrer, C.J. Loland, J.A. Javitch, U. Gether, N-terminal truncation of the dopamine transporter abolishes phorbol ester- and substance P receptor-stimulated phosphorylation without impairing transporter internalization, J. Biol. Chem. 278 (2003) 4990–5000, https://doi.org/10.1074/jbc.M205058200.
[70] L. Tang, R.D. Todd, K.L. O'Malley, Dopamine D2 and D3 receptors inhibit dopamine release, J. Pharmacol. Exp. Ther. 270 (1994) 475–479.
[71] F. Rouge-Pont, A. Usiello, M. Benoit-Marand, F. Gonon, P.V. Piazza, E. Borrelli, Changes in extracellular dopamine induced by morphine and cocaine: crucial control by D2 receptors, J. Neurosci. 22 (2002) 3292–3331, https://doi.org/10.1523/JNEUROSCI.22-08-03293.2002.
[72] P. Sokoloff, B. Giros, M.P. Martres, M.L. Bouthenet, J.C. Schwartz, Molecular cloning and characterization of a novel dopamine receptor (D3) as a target for neuroleptics, Nature 347 (1990) 146–151, https://doi.org/10.1038/347146a0.
[73] R. Maggio, M.J. Millan, Dopamine D2-D3 receptor heterodimers: pharmacological properties and therapeutic significance, Curr. Opin. Pharmacol. 10 (2010) 100–107, https://doi.org/10.1016/j.coph.2009.10.001.
[74] S.D. Dickinson, J. Sabeti, G.A. Larson, K. Giardina, M. Rubinstein, M.A. Kelly, D. K. Grandy, M.J. Low, G.A. Gerhardt, N.R. Zahniser, Dopamine D2 receptor-deficient mice exhibit decreased dopamine transporter function but no changes in dopamine release in dorsal striatum, J. Neurochem. 72 (1999) 148–156, https://doi.org/10.1046/j.1471-4159.1999.0720148.x.
[75] Y. Schmitz, C. Schmauss, D. Sulzer, Altered dopamine release and uptake kinetics in mice lacking D2 receptors, J. Neurosci. 22 (2002) 8002–8009, https://doi.org/10.1523/JNEUROSCI.22-18-08002.2002.
[76] B. Le Foll, J. Diaz, P. Sokoloff, Neuroadaptations to hyperdopaminergia in dopamine D3 receptor-deficient mice, Life Sci. 76 (2005) 1281–1296, https://doi.org/10.1016/j.lfs.2004.09.018.
[77] J.N. Joyce, C. Woolsey, H. Ryoo, S. Borwege, D. Hagner, Low dose pramipexole is neuroprotective in the MPTP mouse model of Parkinson's disease, and downregulates the dopamine transporter via the D3 receptor, BMC Biol. 2 (2004) 22, https://doi.org/10.1186/1741-7007-2-22.
[78] P. Sokoloff, M.P. Martres, B. Giros, M.L. Bouthenet, J.C. Schwartz, The third dopamine receptor (D3) as a novel target for antipsychotics, Biochem. Pharmacol. 43 (1992) 659–666, https://doi.org/10.1016/0006-2952(92)90227-a.
[79] N.M. Richtand, S.C. Woods, S.P. Berger, S.M. Strakowki, D3 dopamine receptor, behavioral, sensitization, and psychosis, Neurosci. Biobehav. Rev. 25 (2001) 427–443, https://doi.org/10.1016/s0149-7634(01)00023-9.
[80] T.E. Koeltzow, M. Xu, D.C. Cooper, X.T. Hu, S. Tonegawa, M.E. Wolf, F.J. White, Alterations in dopamine release but not dopamine autoreceptor function in dopamine D3 receptor mutant mice, J. Neurosci. 18 (1998) 2231–2238, https://doi.org/10.1523/JNEUROSCI.18-06-02231.1998.
[81] J.D. Joseph, Y.-M. Wang, P.R. Miles, E.A. Budygin, R. Picetti, R.R. Gainetdinov, M.G. Caron, R.M. Wightman, Dopamine autoreceptor regulation of release and uptake in mouse brain slices in the absence of D(3) receptors, Neuroscience 112 (2002) 39–49, https://doi.org/10.1016/s0306-4522(02)00067-2.
[82] T.D. Sotnikova, E.V. Efimova, R.R. Gainetdinov, Enhanced dopamine transmission and hyperactivity in the dopamine transporter heterozygous mice lacking the D3 dopamine receptor, Int. J. Mol. Sci. 21 (2020) 8216, https://doi.org/10.3390/ijms21218216.
[83] K.L. Kimmel, F.I. Carroll, M.J. Kuhar, Dopamine transporter synthesis and degradation rate in rat striatum and nucleus accumbens using RTI-76, Neuropharmacology 39 (2000) 578–585, https://doi.org/10.1016/s0028-3908(99)00160-4.
[84] D.E. Rastedt, R.A. Vaughan, J.D. Foster, Palmitoylation mechanisms in dopamine transporter regulation, J. Chem. Neuroanat. 83-84 (2017) 3–9, https://doi.org/10.1016/j.jchemneu.2017.01.002.
[85] C.J. German, G.R. Hanson, A.E. Fleckenstein, Amphetamine and methamphetamine reduce striatal dopamine transporter function without concurrent dopamine transporter relocalization, J. Neurochem. 123 (2012) 288–297, https://doi.org/10.1111/j.1471-4159.2012.07875.x.
[86] E.R. Block, J. Nuttle, J.J. Balcita-Pedicino, J. Caltagarone, S.C. Watkins, S. R. Sesack, A. Sorkin, Brain region-specific trafficking of the dopamine transporter, J. Neurosci. 35 (2015) 12845–12858, https://doi.org/10.1523/JNEUROSCI.1391-15.2015.
[87] G.C. Hadlock, P.W. Chu, E.T. Walters, G.R. Hanson, A.E. Fleckenstein, Methamphetamine-induced dopamine transporter complex formation and dopaminergic deficits: the role of D2 receptor activation, J. Phamacol. Exp. Ther. 335 (2010) 207–212, https://doi.org/10.1124/jpet.110.166660.
[88] J.P. O'Callaghan, D.B. Miller, Neurotoxicity profiles of substituted amphetamine in the C57BL/6J mouse, J. Pharmacol. Exp. Ther. 270 (1994) 741–751.
[89] W. Zhu, J.P. Xu, J.A. Angulo, Induction of striatal pre- and postsynaptic damage by methamphetamine requires the dopamine receptors, Synapse 58 (2005) 110–121, https://doi.org/10.1002/syn.20185.
[90] S. Ares-Santos, N. Granado, I. Espadas, R. Martinez-Murillo, R. Moratalla, Methamphetmine causes degeneration of dopamine cell bodies and terminals of the nigrostriatal pathway evidenced by silver staining, Neuropsychopharmacology 39 (2014) 1066–1080, https://doi.org/10.1038/npp.2013.307.
[91] M.A. Kurian, J. Zhen, S.Y. Cheng, S.R. Mordekar, P. Jardine, N.V. Morgan, E. Meyer, L. Tee, S. Pasha, E. Wassmer, S.J. Heales, P. Gissen, M.E. Reith, E. R. Maher, Homozygous loss-of-function mutations in the gene encoding the dopamine transporter are associated with infantile parkinsonism-dystonia, J. Clin. Invest. 119 (2009) 1595–1603, https://doi.org/10.1172/JCI39060.
[92] F.H. Hansen, T. Skjørringe, S. Yasmeen, N.V. Arends, M.A. Sahai, K. Erreger, T. F. Andreassen, M. Holy, P.J. Hamilton, V. Neergheen, M. Karlsborg, A. H. Newman, S. Pope, S.J. Heales, L. Friberg, I. Law, L.H. Pinborg, H.H. Sitte,

C. Loland, L. Shi, H. Weinstein, A. Galli, L.E. Hjermind, L.B. Møller, U. Gether, Missense dopamine transporter mutations associate with adult parkinsonism and ADHD, J. Clin. Invest. 124 (2014) 3107–3120, https://doi.org/10.1172/JCI73778.

[93] S.R. Jones, R.R. Gainetdinov, M. Jaber, B. Giros, R.M. Wightman, M.G. Caron, Profund neuronal plasticity in response to inactivation of the dopamine transporter, Proc. Natl. Acad. Sci. U.S.A. 95 (1998) 4029–4034, https://doi.org/10.1073/pnas.95.7.4029.

[94] B.K. Gorentla, A.E. Moritz, J.D. Foster, R.A. Vaughan, Proline-directed phosphorylation of the dopamine transporter N-terminal domain, Biochemistry 48 (2009) 1067–1076, https://doi.org/10.1021/bi801696n.

[95] R.A. Vaughan, R.A. Huff, G.R. Uhl, M.J. Kuhar, Protein kinase C-mediated phosphorylation and functional regulation of dopamine transporters in striatal synaptosomes, J. Biol. Chem. 272 (1997) 15541–15546, https://doi.org/10.1074/jbc.272.24.15541.

[96] G.M. Daniels, S.G. Amara, Regulated trafficking of the human dopamine transporter. Clathrin-mediated internalization and lysosomal degradation in response to phorbol esters, J. Biol. Chem. 274 (1999) 35794–35803, https://doi.org/10.1074/jbc.274.50.35794.

[97] H.E. Melikian, K.M. Buckley, Membrane trafficking regulates the activity of the human dopamine transporter, J. Neurosci. 19 (1999) 7699–76710, https://doi.org/10.1523/JNEUROSCI.19-18-07699.1999.

[98] T. Sorkin, M. Miranda, K.R. Dionne, B.R. Hoover, N.R. Zahniser, A. Sorkin, RNA interference screen reveals an essential role of Nedd4-2 in dopamine transporter ubiquitination and endocytosis, J. Neurosci. 26 (2006) 8195–8205, https://doi.org/10.1523/JNEUROSCI.1301-06.2006.

[99] S. Wu, K.D. Bellve, K.E. Fogarty, H.E. Melikian, Ack1 is a dopamine transporter endocytic brake that rescues a trafficking-dysregulated ADHD coding variant, Proc. Natl. Acad. Sci. U.S.A. 112 (2015) 15480–15485, https://doi.org/10.1073/pnas.1512957112.

[100] R.R. Gainetdinov, R.T. Premont, L.M. Bohn, R.J. Lefkowitz, M.G. Caron, Desensitization of G protein-coupled receptors and neuronal functions, Ann. Rev. Neurosci. 27 (2004) 107–144, https://doi.org/10.1146/annurev.neuro.27.070203.144206.

[101] E.Y. Cho, D.I. Cho, J.H. Park, H. Kurose, M.G. Caron, K.M. Kim, Roles of protein kinase C and actin-binding protein 280 in the regulation of intracellular trafficking of dopamine D3 receptor, Mol. Endocrinol. 21 (2007) 2242–2254, https://doi.org/10.1210/me.2007-0202.

[102] W. Poewe, K. Seppi, C.M. Tanner, G.M. Halliday, P. Brundin, J. Volkmann, A. E. Lang, Parkinson disease, Nat. Rev. Dis. Primers 3 (2017), 17013, https://doi.org/10.1038/nrdp.2017.13.

[103] A.G. Szmulewicz, F. Angriman, C. Samamé, A. Ferraris, D. Vigo, S.A. Strejilevich, Dopaminergic agents in the treatment of bipolar depression: a systematic review and meta-analysis, Acta Psychiatr. Scand. 135 (2017) 527–538, https://doi.org/10.1111/acps.12712.

[104] P. Huot, S.H. Fox, J.M. Brotchie, Dopamine reuptake inhibitors in parkinson's disease: a review of nonhuman primate studies and clinical trials, J. Pharmacol. Exp. Ther. 357 (2016) 562–569, https://doi.org/10.1124/jpet.116.232371.

[105] K.J. Miller, B.J. Hoffman, Adenosine A3 receptors regulate serotonin transport via nitric oxide and cGMP, J. Biol. Chem. 269 (1994) 27351–27356.

[106] J.M. Launay, D. Bondoux, M.J. Oset-Gasque, S. Emami, V. Mutel, M. Haimart, C. Gespach, Increase of human platelet serotonin uptake by atypical histamine receptors, Am. J. Physiol. 266 (1994) R526–536, https://doi.org/10.1152/ajpregu.1994.266.2.R526.

[107] S. Apparsundaram, A. Galli, L.J. DeFelipe, H.C. Hartzell, R.D. Blakely, Acute regulation of norepinephrine transport: I. Protein kinase C-linked muscarinic receptors influence transport capacity and transporter density in SK-N-SH cells, J. Pharmacol. Exp. Ther. 287 (1998) 733–743.

[108] M.L. Beckman, E.M. Bernstein, M.W. Quick, Multiple G protein-coupled receptors initiate protein kinase C redistribution of GABA transporters in hippocampal neurons, J. Neurosci. 19 (RC9) (1999) 1–6, https://doi.org/10.1523/JNEUROSCI.19-11-j0006.1999.

[109] P.M. Carvey, S.O. McGuire, Z.D. Ling, Neuroprotective effects of D3 dopamine receptor agonists, Parkinsonism Relat. Disord. 7 (2001) 213–223, https://doi.org/10.1016/s1353-8020(00)00061-4.

[110] C. Li, Y. Guo, W. Xie, X. Li, J. Janokovic, W. Le, Neuroprotection of pramipexole in UPS impairment induced animal model of Parkinson's disease, Neurochem. Int. 35 (2010) 1546–1556, https://doi.org/10.1007/s11064-010-0214-3.

[111] M. Kim, S. Lee, J. Cho, G. Kim, C. Won, Dopamine D3 receptor-modulated neuroprotective effects of lisuride, Neuropharmacology 117 (2017) 14–20, https://doi.org/10.1016/j.neuropharm.2017.01.022.

[112] P. Su, F. Liu, A peptide disrupting the D2R-DAT interaction protects against dopamine neurotoxicity, Exp. Neurol. 295 (2017) 176–183, https://doi.org/10.1016/j.expneurol.2017.05.010.

[113] D.M. Rosenbaum, S.G. Rasmussen, B.K. Kobilka, The structure and function of G-protein-coupled receptors, Nature 459 (2009) 356–363, https://doi.org/10.1038/nature08144.

[114] M. Jin, C. Min, M. Zheng, D.I. Cho, S.J. Cheong, H. Kurose, K.M. Kim, Multiple signaling routes involved in the regulation of adenylyl cyclase and extracellular regulated kinase by dopamine D(2) and D(3) receptors, Pharmacol. Res. 67 (2013) 31–41, https://doi.org/10.1010/j.phrs.2012.09.012.

[115] N.M. Urs, M.G. Caron, The physiological relevance of functional selectivity in dopamine signalling, Int. J. Obes. Suppl. 4 (Suppl 1) (2014) S5–8, https://doi.org/10.1038/ijosup.2014.3.

[116] M.N. Urs, S. Bido, S.M. Peterson, T.L. Daigle, C.E. Bass, R.R. Gainetdinov, E. Bezard, M.C. Caron, Targeting β-arrestin 2 in the treatment of L-DOPA-induced dyskinesia in Parkinson's disease, Proc. Natl. Acad. Sci. U. S. A. 112 (2015) E2517–2526, https://doi.org/10.1073/pnas.1502740112.

[117] W. Xu, X. Wang, A.M. Tocker, P. Huang, M.E. Reith, L.Y. Liu-Chen, A. B. Smith 3rd, S. Kortagere, Functional characterization of a novel series of biased signaling dopamine D3 receptor agonists, ACS Chem. Neurosci. 8 (2017) 486–500, https://doi.org/10.1012/acschemneuro.6b0022.